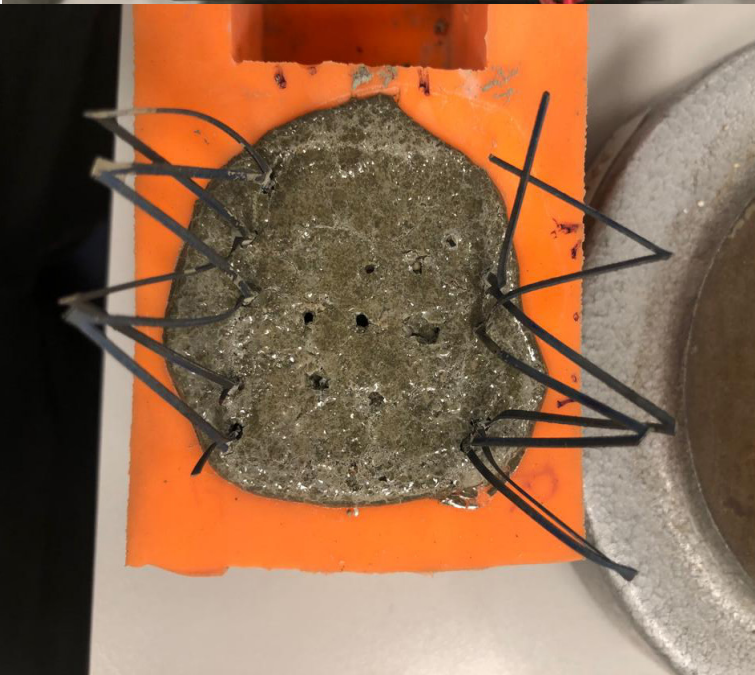
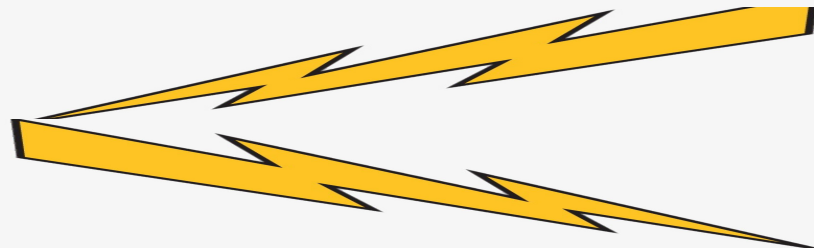


MSc Thesis Electric Curing Of Cement Mortar

Arjun Raghavan - 5122864





Delft University of Technology

Faculty of Civil Engineering and Geosciences

Electric Curing of Cement Mortar

Name: Arjun Raghavan

Studentnr: 5122864

Date: 08/02/2023

Supervisors:

Dr.D.A.Dessi Koleva

Dr.Oğuzhan Copuroglu

Dr. Peyman Taheri

Dr.Emanuele Rossi

Cover Image from: https://www.pngkey.com/detail/u2r5u2e6e6w7o0r5_nature-gold-lightning-bolt-png/

Contents

1	Introduction	8
1.1	Scope and Objectives	9
1.2	Layout of thesis	9
2	Literature Review	10
2.1	General Introduction	10
2.2	Hydration of Cement	10
2.3	Curing at Elevated Temperatures and Accelerated Curing Methods	11
2.4	Steam Curing	12
2.5	Accelerating Admixtures	13
2.6	Retarding Admixtures	13
2.7	Water Reducers	14
2.8	Electrical Properties of Mortar	14
2.9	Electric curing	14
2.9.1	Curing Regimes	15
2.9.2	Polarisation	15
2.9.3	Mechanism of Electric Curing	16
2.10	Effects of Electric Curing on Concrete Properties	17
2.10.1	Compressive Strength	17
2.10.2	Setting Time	17
2.10.3	Porosity	17
2.10.4	Ettringite Formation	17
2.11	Summary and Outlook of Literature Study	18
3	Experimental Study	19
3.1	Outline of the Experimental Study	19
3.2	Sample Preparation	19
3.3	Curing Setup	22
3.3.1	Direct Current	24
3.3.2	Alternating Current	26
3.3.3	Pulsed DC	27
3.4	Behaviour of Voltage and Current	30
3.4.1	Direct Current	30
3.4.2	Alternating Current	30
3.4.3	Pulsed Direct Current	32
4	Testing Specimens	34
4.1	Outline	34
4.2	Setting Time	34
4.3	Modified Vicat	35
4.4	Compression Test (1D, 3D and 7D)	37
4.5	Resistivity Measurement	37

5	Results	38
5.1	Overview of results	38
5.2	Setting Times	38
5.2.1	Direct Current Setting Times	38
5.2.2	Alternating Current Setting Times	40
5.2.3	Alternating Current- 15V (Accelerator) Setting Times	41
5.2.4	Pulsed Direct Current Setting Times	42
5.2.5	Compressive Strength	43
5.2.6	Setting Time Vs Resistivity- Direct Current	46
5.2.7	Setting Time vs Resistivity- Alternating Current	47
5.2.8	Setting Time Vs Resistivity- Pulsed Direct Current	49
5.2.9	Temperature-Direct Current	50
5.2.10	Temperature-Alternating Current	51
5.2.11	Temperature vs Resistivity	52
5.2.12	Electrical Data- Charges and Power	53
6	Discussions	57
6.1	Validity of the Experimental Setup	57
6.2	Setting Times	57
6.2.1	Direct Current	57
6.2.2	Pulsed Direct Current	59
6.2.3	Alternating Current	60
6.3	Compressive Strength	61
6.3.1	Direct Current	61
6.3.2	Pulsed Direct Current	61
6.3.3	Alternating Current	61
6.4	Resistivity	62
6.4.1	Direct Current and Pulsed Direct Current	62
6.4.2	Alternating Current	62
6.5	Electrical Data Comparisons	63
7	Conclusions	64
8	Recommendations	66
9	Appendix-A- Mixing procedure	68
10	Appendix-B	69
10.1	Pulse Direct Current- Compressive Strength	69
10.2	Pulse Direct Current- Pulse data	69
11	Appendix-C- Setting time vs resistivity	71

List of Figures

1	Steam curing cycle [28]	12
2	Ti-MMO Mesh	20
3	Mould setup for the setting time test	20
4	Cube specimen subjected to electric curing	21
5	Direct current curing setup	24
6	Alternating current curing setup	26
7	Flowchart of Pulsed direct current curing setup	28
8	Voltage and current trend for $10A/m^2$	30
9	Voltage and current trend for 10V	31
10	Voltage and current trend for $10A/m^2$ pulsed direct current	32
11	Voltage and current trend for $10A/m^2$ pulsed direct current	33
12	Voltage and current trend for $10A/m^2$ pulsed direct current	34
13	Box mould without electrodes	35
14	Box mould with electrodes	36
15	Setting time curves of samples subjected to direct current regimes	39
16	Setting time curves of samples subjected to alternating current regimes	40
17	Setting time of cement mortar with chemical accelerator subjected to 15V AC	41
18	Setting time curves of samples subjected to pulsed direct current regimes	43
19	1-day Compressive strength of all the curing regimes	44
20	3-day compressive strength of all curing regimes	45
21	7-day compressive strength of all the curing regimes	46
22	Setting time and resistivity development with time - Control and DC cured specimen	47
23	Setting time and resistivity development with time - Control and AC cured specimen	48
24	Setting time and resistivity development with time - Control and pDC cured specimen	49
25	Temperature curves of the selected DC regimes	50
26	Temperature curves of AC regimes	51
27	temperature vs resistivity development for DC cured samples	52
28	temperature vs resistivity development for AC cured samples	53
29	Charge Comparison- DC and pDC regimes	54
30	Power Comparison between DC,AC and pDC regimes	55
31	20 A/m ² samples prepared for a 3-day compressive strength test	58
32	Control samples (without application of current) prepared for a 3-day compressive strength test	59
33	5 A/m ² pDC voltage and current pulse	69
34	10 A/m ² pDC voltage and current pulse	70
35	20 A/m ² pDC voltage and current pulse	70
36	Setting time and resistivity development with time - Control and DC cured specimen-Trial 2	71
37	Setting time and resistivity development with time - Control and DC cured specimen-Trial 3	71
38	Setting time and resistivity development with time - Control and AC cured specimen-Trial 2	72

39	Setting time and resistivity development with time - Control and AC cured specimen- Trial 3	72
40	Setting time and resistivity development with time - Control and pDC cured specimen- Trial 2	73
41	Setting time and resistivity development with time - Control and pDC cured specimen- Trial 3	73

List of Tables

1	CEM-I-42.5N - Chemical Composition	19
2	Particle size distribution of fine aggregates	19
3	Material weight	21
4	Fine aggregate weight distribution	21
5	Direct current regimes	25
6	Alternating current regimes	27
7	Pulsed Direct Current regimes	29
8	Setting times obtained from modified Vicat apparatus testing for the DC regimes	38
9	Setting times obtained through modified vicat apparatus for AC regimes AC regimes	40
10	Setting times obtained through modified vicat apparatus for AC+accelerator . .	42
11	Setting times obtained from modified vicat apparatus for pDC regimes	42
12	Setting time and resistivity from 23	49
13	The amount of charge the DC/pDC regime supplies at the end of the 6-hour curing cycle	55
14	The amount of charge the DC/pDC regime supplies at the end of the 6-hour curing cycle	56

Abstract

In this research, the effect of curing with different types of current, current densities/voltage intensity on mortar is studied. The main objective is to explore the outcomes of electric curing on the setting time of CEM-I mortar. For achieving the main objective, an electrical curing setup is designed to accommodate curing with direct current, alternating current and pulsed direct current and the conventional vicat apparatus and its test procedure are modified in order to carry out the testing while a sample is being cured with current. Additionally, the effect of passing current on material properties such as compressive strength and resistivity is also studied. The temperature development during the curing process has also been monitored in the research. The electric charge and power calculation are done, for possible current/voltage regimes. The experiments revealed that the setting time can be altered by electrical curing of CEM-I mortar. The influence of electric curing for the chosen curing period is not significant as revealed from the compressive strength testing while the development of resistivity and temperature reveals that there is a correlation between these two properties. The effect of electric power applied to a sample is reflected in the results of the setting times. In the last chapter the findings of the study are summarised and recommendations, keeping in mind the possibility of expanding research in this field of study, have been made.

Acknowledgement

This has been the most challenging phase of my life so far and to say that I managed to overcome everything on my own would not be fair.

Firstly, I would like to thank my committee, Dr.Dessi Koleva for her guidance and support throughout the course of this master thesis. The reason I took interest in material sciences is because of Dr.Oğuzhan Copuroglu. I am glad that I was able to interact and work with Oguzhan and improve my knowledge on forensic studies. I would like to thank Dr.Peyman Taheri for his advices to make my master thesis better. Without Dr.Emanuele Rossi, my stint at TU Delft would not have been possible. More than a committee member, he has been my best friend and mentor, helping me out both in my personal and professional life. I hope not to leave him anytime soon and I am waiting for my trip to Italy after I finish my course here at TU Delft. My master thesis required a lot of inputs with regards to setting up electrical equipment and this would not have been possible without Kees van Beek. I had so much fun during our discussions and I am pretty sure that no other master student would have spent this much time with Kees. Every time I went to Kees with a problem he would always make sure to sort it out so that it does not disrupt my lab work. I also thank Sam Reus for helping me out with my lab work. I never had to wait for Sam, he somehow got things arranged for me even during the holiday periods. My days at the laboratory during the lockdowns, and of course, even after the lockdown period were fun because of Maiko. He has been a good friend always around to cheer me up whenever I am down. Thank you, Maiko. I would like to thank John, Arjan, Ton for helping me out in the lab and for the interactions that we have had whenever we had the time. I am lucky to have met and interacted with the PhD candidates at microlab and I would like to thank them for their interactions.

Coming to The Netherlands was a big step for me personally and the transition of coming from India was only possible because of Sitra aunty, Sameer and Mickey with whom I stayed for almost 3 years now. I always attribute my progress in life to my family and friends and this would be no different.

Without Karthi, Ganesh, Mukil, Dharshan, Roshan, Hem, Medha, Navin, Sanjay my life at TU Delft and these 3 years would have been impossible. My friends back at India, now spread across all over the world, have always had my back and I am forever indebted for the love I have received from them. Last, but never the least, I thank Appa, Amma, my sister and my grand parents for the support and affection.

Arjun Raghavan

1 Introduction

Increasing productivity of pre-fabricated elements at factories, emergency in-situ repair works, and 3D printing of concrete has led to the need for modifying the mix designs of concrete according to each purpose. With recent developments in the concrete industry, accelerated curing methods are gaining popularity: these methods are adopted in fields that require faster execution of concrete works. Electric curing is one such method used to increase productivity at factories by accelerating the curing period of concrete elements. It involves passing current through the concrete specimen to make use of the concrete mix's resistance to current flow in order to generate heat, this mechanism is also known as Joule's heating effect.

The acceleration of the curing process has both positive and negative side effects: accelerated curing could increase the early-age compressive strength of the mixture while, on the other hand, it may increase its porosity as well as cause delayed ettringite formation. The negative side effects related to accelerated electric curing can be countered by applying different electric current regimes/types for the curing process [16]. Conventionally alternating current has been used for the electric curing process. However, similar effects such as a gain in compressive strength have also been reported by Susanto et al. [35]. in the study of the effects of stray current on hardening and hardened cement-based materials.

Direct current is mainly used in concrete technology for cathodic protection, cathodic prevention, and cathodic realkalization, wherein current densities ranging from $1\text{mA}/\text{m}^2$ to $2000\text{mA}/\text{m}^2$ are applied. Experimental and modelling results show that an increase in early-age compressive strength is also possible using direct current if the intensity is increased [35]. Along with alternations in material characteristics, polarisation and hydrogen evolution at the electrodes may occur during the application of direct current for cathodic protection. The downside of using direct current has recently been countered by the pulsed direct current [18]. Most of the research on accelerated curing methods focused on quantifying compressive strength development under different electric curing regimes. However, it must be pointed out that a potential advantage of using such curing methods is the modification of setting time due to the current application. This aspect has not been comprehensively investigated yet, and insights about accelerating setting time by application of current would have applications in fields such as 3D printing since the 3D-printed mixture needs to be sufficiently set (and hard) to print a subsequent mixture layer on its top. Uygunoğlu et al.[40] have reported a decrease in setting time when applying alternating current through the sample, and the temperature evolution during the current application to the sample has been correlated with the setting time showing higher temperature evolution results in a decrease in setting time.

Besides the previous studies focused on the effects of stray current on cementitious material properties, assessment of the setting time of samples subjected to AC-electric curing, insights into the effect of direct current on the setting time and assessing setting of samples subjected to electric curing using vicat testing has not been investigated. Thus, the present study is focused on experimentally verifying the changes to setting time due to the application of different types and intensities of current, if there are any, while also reporting the influence of application of current through properties, such as compressive strength, resistivity, that have been reported in previous studies [24, 44, 6].

1.1 Scope and Objectives

The main objective of this research was to investigate the effects of different current types and current/voltage intensities on fresh cement mortar. The following aspects were studied to answer the main objective:

- Assessment of setting time of cement mortar subjected to different current types and intensities
- Effects of direct current, alternating current and pulsed direct current on cement mortar properties, such as compressive strength and resistivity.

The results from this work aim to contribute to understanding the positive or negative impact of using electric current on cementitious materials.

1.2 Layout of thesis

The present research consists of 7 chapters.

Chapter 1 briefly introduces accelerated curing methods and their applications and side effects. In this chapter, the scope and objectives of the present research are also highlighted.

Chapter 2 consists of a literature study on the hydration of cement, curing at high temperatures, accelerated curing methods, electric curing of concrete and the stages involved in designing curing cycles, electrical properties of concrete, mechanisms of accelerators and retardants used for altering the setting times of concrete mixes. The effects of electric curing on concrete samples are also discussed.

Chapter 3 consists of details regarding sample preparation and the construction of the curing setup for different types of current. The current and voltage behaviour of the different curing regimes in the presence of the mortar samples are also discussed.

Chapter 4 deals with the tests carried out on the prepared samples, such as the setting time test, compression test, resistivity measurement and temperature measurement. The chapter also provides details on how the conventional vicat apparatus was modified to suit the requirements of the current study.

Chapter 5 consists of the compilation of results obtained by carrying out the experiments required in this study. The results are graphically represented, and an overview of the results is presented. In Chapter 6, a discussion of the results presented in chapter 5 is formulated. The validity of the curing setup, alterations in the setting times, and the trend of compressive strength and resistivity with age are discussed in this chapter.

Chapter 7 comprises the conclusions from the present study, the recommendations that should be taken into account for future research and the limitations related to the applied methodologies.

2 Literature Review

2.1 General Introduction

With its versatility in the construction field and availability, concrete is by far the most used construction material in the world. Concrete is a composite material made primarily from a cementing/binding medium, aggregates, water and other embedded materials. Depending on the binding medium, concrete is classified into various types. Ordinary Portland cement, being one of those, is categorised as a hydraulic cement type where the hydration products (mainly Calcium Silicate Hydrates (C-S-H) and Calcium hydroxide (CH)) are formed as a result of the interaction of calcium silicates with water and are stable in an aqueous medium [21][26]. As of 2006, approximately 8% of anthropogenic CO₂ emissions were due to cement production. In the coming years, cement production is expected to reach approximately 5 billion tonnes to meet global requirements, with each ton of cement producing 0.65-0.95 tons of CO₂ (as reported in 2006) [25]. Substituting portland cement with new alternatives might lead to a 20%-80% reduction of CO₂, depending on the scenarios. Though alternatives are the way to move forward, for the time being, it is essential to make efficient use of cement by producing good-quality concrete elements with it [25][5]. Good quality concrete, on a rudimentary level, is defined by two fundamental criteria: (i) its fresh state properties like the ease of transportation, casting, and (ii) its hardened state properties like compressive strength [28]. Several parameters determine how good a concrete mix is in its performance, with curing during the early stages being one of those parameters [32].

The process involved in stimulating cement hydration and strength development of concrete is capped under the term 'Curing' in concrete technology. The improved properties of concrete that come with proper curing are brought about by temperature and moisture regulation during the initial stages (fresh state of concrete). It is well known that however good the mix of the concrete is, the quality of the final product, i.e., the concrete element for which the mix is used, is subject to proper placing and curing methods [28]. In addition to the conventional curing methods, quite a few options involve accelerating the curing process by elevating the temperature internally and externally. This increase in curing temperature during the early stages of hydration can accelerate the hydration processes and strength gain. Early strength gain of concrete elements is required to ensure profitable outcomes in the pre-cast industry [28, 16].

The execution of accelerated curing can be carried out through a physical process such as applying heat. Steam curing, Steam injection, oil heating, and water heating are examples of curing methods involving heat application through an external heat source. On the other hand, electric curing is a method where the heat required for accelerated curing is obtained from within the concrete by passing an electrical current through the sample (Ohmic heating) [16].

2.2 Hydration of Cement

The raw materials used in the production of Portland cement mainly consists of Lime, Silica, Alumina and iron oxide. In the kiln, where high temperatures are maintained, these compounds interact with each other and result in the formation of these 4 major constituents in Portland cement clinker: *i*)C₃S *ii*)C₂S *iii*)C₃A *iv*)C₄AF. C₃S and C₂S are responsible for the strength gain in the cement paste, C₃A plays a role in the strength gain during the early stages and helps in

the fusion of lime and silica during the cement production. When Portland cement with gypsum gets hydrated, the following reactions occur [45] [29]:

1. There is hydration of alumina and alite for a short period which occurs initially with a high reaction rate. The sulphates from the cement clinker and the gypsum goes into solution and starts forming an amorphous gel containing sulphates, silica, alumina and lime. This dissolution period is followed by a dormant period. This dissolution period also involves formation of small crystals of ettringite.
2. Alite hydration produces Calcium-Silica hydrates and calcium hydroxide which are sized up to 10 μ m. This occurs at around 6 – 12 hours, where the concrete has set but has considerably low strength.
3. Cement reacts in 2 ways: i) Dissolution occurs at the surface of the cement grain, with the dissolved particles passing through the coating of the fluid and reprecipitating in the large water-filled gaps between the cement grains. ii) CSH forms within the volume contained by the cement particle.
4. After a day, the sulphates that were present are almost used up but the aluminate phase still undergoes hydration. This depletion causes formation of mono-sulphates. After a few more days, the ettringite starts to decompose to form mono-sulphates as well. The large water filled pores are occupied by CSH and CH (calcium hydroxide). The cement paste becomes denser.
5. From 3 days onwards, alite reaction becomes depleted and belite contributes more towards strength gain. Overall reaction rates get slower with increase in time. Most of the available sulphates are in mono-sulphate form.

The above products of hydration forms one of the three phases in concrete/mortar, the hydrated cement phase. The other 2 are: The interfacial transition zone and the aggregate phase [26].

2.3 Curing at Elevated Temperatures and Accelerated Curing Methods

The main objective of curing is to keep the concrete saturated or at least partially saturated until the water-filled pores in the cement paste are replaced with products of hydration. Thus, the need for curing is to avoid the loss of water from the capillaries while at the same time replacing the water that is lost as a result of self-desiccation. Usually, self-desiccation occurs in sealed concrete samples at w/c ratio of less than about 0.5. This study focuses more on accelerated methods rather than the conventional methods of curing such as oiling and wetting, using an impermeable membrane or waterproof reinforced paper or plastic sheets.

The initial rate of strength development is significant, and the strength at the later stages is less in elements cured at higher temperatures [28]. This enhancement in strength is capitalised for fabrication at pre-cast, prestressed concrete element factories and in places where the formwork needs to be removed earlier than required, as in some in-situ scenarios[42][31]. Studies show that increasing the curing temperatures, even under regulated conditions, can negatively affect the durability of the cured elements [40][4]. Accelerated curing works under the assumption that

evaporation of the capillary water [28] is advantageous for strength gain when the capillaries are still allowed to collapse. This evaporation results in a reduction of the effective water-cement ratio. When the water-cement ratio is reduced, the porosity decreases and the resultant microstructure is rendered denser when compared to samples without this controlled evaporation [28]. To better understand the working of different accelerated curing methods: i) steam curing and ii) curing with a chemical accelerator are discussed.

2.4 Steam Curing

In this accelerated curing method, the increase in the rate of strength gain is obtained by increasing the curing temperature with the help of steam. Steam is applied to the concrete element while the concrete elements are transported through a conveyor belt within special chambers or tunnels [29, 39]. The influence of high temperatures during the early stages of setting/hardening has detrimental effects on concrete properties, so heat application through steam should be controlled. For the application of higher temperatures steam to account for delivery or completion deadlines, there should be an optimal delay period for the concrete mix so that the elements can handle the internal thermal stresses [26, 28]. With an optimal delay period of 3-5 hours (primarily the initial set of a concrete mix), the temperature can be increased up to 66°C - 82°C . While it is necessary to increase the temperature at a controlled rate, the cooling rate of the elements should also be gradual. If this is not the case, there is a possibility of a temperature gradient that might cause the cracking of the cured elements. Figure 1 shows the stages involved and the corresponding temperatures in a sample steam curing cycle

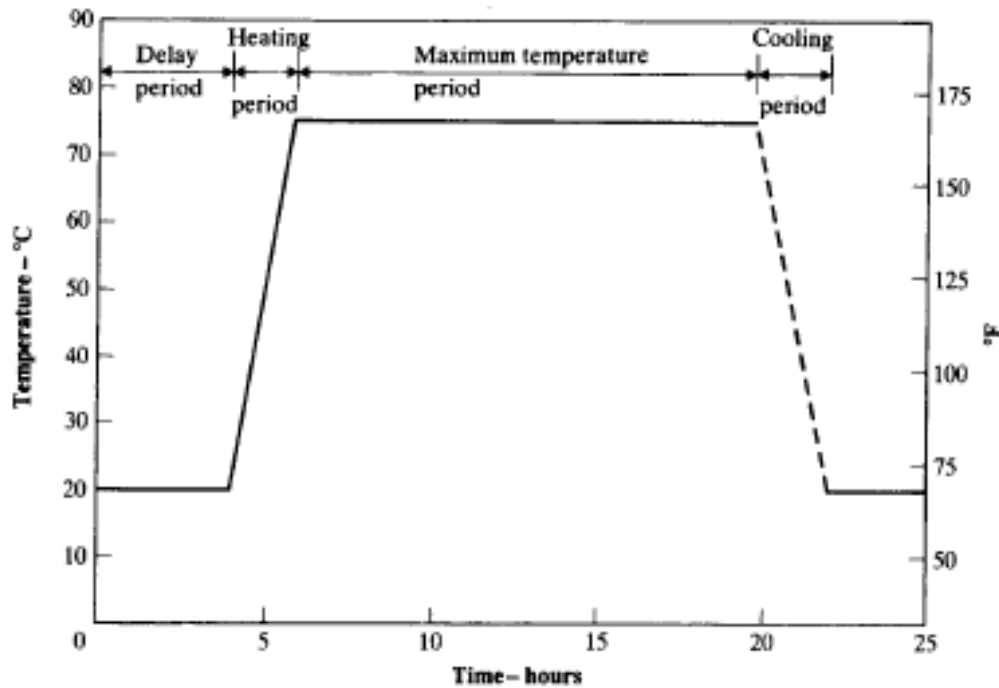


Figure 1: Steam curing cycle [28]

From figure 1, for accelerated curing under the application of steam, there is a delay period,

heating period, retention period and cooling period [26, 28, 45, 16]. These stages in steam curing are similar to the electric curing method.

2.5 Accelerating Admixtures

An accelerating admixture increases the rate of hydration (setting time accelerator) and increases the early age strength of concrete. The possibility of an accelerator to affect both setting and strength should not be neglected [15]. One of the commonly used chemical accelerators are Calcium chloride (CaCl_2). Calcium chloride acts as both a setting time and hardening accelerator for ordinary Portland cement (OPC) and accelerates the reaction between tricalcium aluminate (C_3A) and gypsum along with facilitating the hydration of C_3S [36][19]. It should also be noted that chloride-based accelerators have a potential to cause drying shrinkage, reinforcement corrosion, discoloration and an increase in possibilities of scaling [8]. Since, CaCl_2 promotes reinforcement corrosion its usage is being reduced and even stopped in countries like UK and other alternatives such as nitrate and nitrite salts are used as they have a lesser corrosive effect on the reinforcements [15]. The accelerating effect depends on the cation and anion in the accelerating admixture and are ranked as follows:

$$\text{Ca}^{2+} > \text{Sr}^{2+} > \text{Ba}^{2+} > \text{Li}^+ > \text{K}^+ > \text{Na}^+ > \text{Cs}^+ > \text{Rb}^+ \quad (2.1)$$

$$\text{Br}^- > \text{Cl}^- > \text{SCN}^- > \text{I}^- > \text{NO}_3^- > \text{ClO}_4^- \quad (2.2)$$

The acceleration effect increases with increase in charge and decrease in the size of the ion. Thus, Ca^{2+} is more effective than any other cation[15].

Calcium nitrate acts mainly as a set accelerator rather than a hardening accelerator with its performance based on the type of cement used. It is mainly used in places where reinforcements are used in concrete in order to reduce the possibility of corrosion. When $\text{Ca}(\text{NO}_3)_2$ goes into solution, the anionic species (NO_3^-) results in the formation of AFm phases. It has been found that these AFm phases resulted in the increased formation of ettringite. In the presence of calcium nitrate as an accelerator, the heat flow during the induction period increases, hence promoting the occurrence of the acceleration period and causing the fast hydration of C_3S . Calcium hydroxide (CH) precipitation also happens during the early stages of hydration. This is because of super saturation of the solution with Ca^{2+} [43, 14] was found that efficiency of $\text{Ca}(\text{NO}_3)_2$ increased with increase in the belite (C_2S) content in cement [37][2][7].

2.6 Retarding Admixtures

Thomas et al. [38] report that retardation occurs from the surface adsorption of a retardant on a hydration product. When a retarder like sucrose is used, the poisoning of hydration product surfaces tends to leave the Ca^{2+} ions along with silicon, hydroxyaluminate and hydroxoferrite ions at concentrations that would not be present if there was equilibrium in the solution. When there was treatment with sucrose, the sucrose anion gets incorporated onto the surface of a CSH or CH particle, thus inhibiting the growth of the particle further [38]. In conclusion, the retarder readily adsorbs onto the CSH surface and has a high affinity for forming complexes with Ca^{2+} ions in the solution, which retards the setting by delaying the formation of hydration products [36].

2.7 Water Reducers

Water reducers prevent the flocculation of cement particles by increasing the zeta potential on the surface of particles creating a repulsion between particles having similar charge and magnitude. They tend to have more affinity to be in the liquid phases rather than combining with solids to form a chain of hydration products. Reduction in flocculation of cement particles can also be attributed to steric hindrance, where the adsorption of a non-ionic polymer might result in weaker forces of attraction between those particles [36].

2.8 Electrical Properties of Mortar

Electrical resistivity is defined as the ability of a material to resist the flow of electricity. The electrical resistivity is a geometrical-independent material property, i.e., the resistivity of a material would approximately be the same value irrespective of its shape and size. Concrete is a heterogeneous mixture [29, 1] where conduction of current can be of two types: i) electronic conduction - conduction through conductive materials embedded in concrete such as fibres, ii) ionic conduction - conduction through ions present in the pore solution. Without the presence of embedded materials for conduction, the ions in the pore liquid carry the electrical current. More pore water and larger pore size with high connectivity and lower tortuosity results in lower resistivity values. The resistivity values tend to increase as concrete sets. This increase is due to the densification of the matrix as a result of the formation of hydration products [31]. The electrical resistivity of concrete is governed by the microstructure of the matrix, pore structure, porosity, pore size distribution, the concentration of ions and their mobility in the pore solution. These factors are, in turn, influenced by water-cement ratio, cement type, degree of hydration, presence of supplementary cementitious materials, curing, and environmental conditions [32, 4, 46]. The type of cement that is being used has an impact on pore structure and pore water chemistry [10]. Sengul et al. [32] reported that OPC has higher resistivity values during the early ages, and an increase in age limits the increase in resistivity when compared to mixtures produced with pozzolanic materials. The resistivity also increased with an increase in aggregate content. Mixtures containing 16-32mm aggregates had higher resistivity than mixtures with aggregates of size range 0-4mm. The water-cement ratio, which also has a profound effect on the microstructure, is inversely proportional to the electrical resistivity, i.e., the higher the water-cement ratio lower the electrical resistivity. The increase in resistivity due to higher w/c ratios can be attributed to the coarser and more continuous pore structure. Temperature changes also affect electrical resistivity, where a temperature increase decreases resistivity and vice-versa. With an increase in temperature, the viscosity of fluid decreases and increases the mobility of ions in the pore solution resulting in a decrease in resistivity. Since the pore water acts as an electrolyte with lower resistivity when compared to the solid matrix, the moisture content is an important factor affecting the electrical resistivity of concrete. The electrical resistivity increases with a decrease in moisture content and vice versa [43].

2.9 Electric curing

Concrete samples are subjected to current flow, or voltage potential is set across them in this curing method internally or externally. This application of the current through the concrete

samples increases the concrete's temperature and generates heat within the concrete samples. Electric curing can be categorised into two types: The semi-Direct curing method uses cheaper heating elements or reinforced concrete reinforcement as heating elements. The voltage applied in this method is low due to the restrictions posed by the 'heating element'. When reinforcements are used to supply current to the sample, the area of concrete that can be heated is comparatively low when heating elements or electrodes. Direct curing uses external electrodes to pass current through the concrete. When this is done, the concrete acts as a heating resistor—in other words, the concrete experiences ohmic heating [12]. Direct electric curing is used for pre-cast elements and repairs with low environmental temperatures [16, 24]. In any accelerated curing method, the optimum range of temperatures would be between 60°C - 80°C , [24, 39, 20, 40]. The duration of exposure to a specific temperature range, the mix type, and the rate of increase of curing temperature are some parameters to be considered for an accelerated curing method. In the case of electric curing, the temperature variance is brought about by varying the current or the voltage across the samples [40, 34].

2.9.1 Curing Regimes

The current regimes depend on the current type used for the electric curing process. Electric curing is usually done under $1\text{A}/\text{m}^2$ to $70\text{A}/\text{m}^2$ [15, 36], or the curing cycle is calculated based on the power required to increase and maintain the temperature to accelerate curing [16]. If the current type is direct current, there is a constant current source, meaning that the current is kept constant, and the voltage is not regulated as the resistance of cementitious materials varies with time. Electric curing mainly utilises AC as the common current type to counter the effects of using DC, predominantly polarisation, in the presence of a dipole like water [13]. The power source used for AC is the power outlet we generally have in buildings but the voltage is stepped down using a transformer and regulated with a variac, and the necessary voltage required is used in the curing process [16, 13]. Uygunoğlu et al. [40] reported that 40V and 60V are the optimum voltage intensities for curing a concrete element of size $10\text{cm} \times 10\text{cm} \times 35\text{cm}$ considering the strength development and setting times of mixes with varying cement content.

2.9.2 Polarisation

Polarisation is the change in potential from its equilibrium state [cite]. Polarisation occurs when an electrolyte is subjected to the flow of current. The polarisation of the electrodes occurs due to the transfer of ions from the electrolytic solution to the electrode. Due to this, a charge build-up near the electrode's surface resists the current flow, resulting in an added potential difference. This polarisation effect of charge build-up near the electrode generates a back-EMF [13]. When direct current is passed through an electrolyte, an EMF (electromotive force) is developed between the electrode and the electrolyte, which opposes the current flow and is called back-EMF. EMF is the electric potential between two electrodes in a cell. This local electric field formed due to polarisation causes an increase in resistivity measurements with time [43]. This measurement discrepancy can be countered by using alternating current, provided that the magnitude of positive and negative cycles of alternating current is the same with no phase shift. The magnitude of the AC cycle (positive and negative) changes depending on the AC frequency [14]. Along with the polarisation of the electrodes, the polarisation of the bulk electrolyte can

also occur due to aligned charged particles and dipole molecules in the direction of the current flow [13].

2.9.3 Mechanism of Electric Curing

The current need not be applied to the samples for the entirety of the chosen curing cycle period. Minimal time and energy should be critical features of a curing process. Thus, the curing revolves around a heating cycle, which consists of the following stages:

1. Pre-heat storage period
2. Heating up period
3. Isothermal period
4. Cooling period

In the pre-heat storage period, the cementitious element is allowed to undergo its natural curing to ensure sufficient resistance to the forces exerted when there is heat development due to the application of current. These forces are generated due to the difference in thermal expansion coefficients of the materials in the cementitious material. When the mixes are heated up without the pre-heating storage time, it results in a sample with a porous microstructure and a lower compressive strength. The current can be applied as soon as the mix is cast in the moulds in electric curing. But it has to be kept in mind that the moulds should not be excessively heated as soon as the mix is placed in the mould. Since the heat is generated from within the concrete during its fresh state, the thermal expansion of entrapped air is countered as the mix is still in its fluid-plastic stage. It is always best if the elements/samples are allowed to follow their natural cure initially before heat administration [16, 13]. Usually, the concrete specimen is allowed to undergo natural curing for 3-5 hours before the heat treatment [9].

This stage is followed by the heating cycle involving the heating up of the specimen by the passage of current through it. The duration and the intensity of heating depends on the equipment, method of heating, thermal properties of the mix and mould construction. The heating is done only for a few hours, which is the reason for using this curing method. The heating is gradually started at a slower rate, and the heating rate can be increased but should not exceed $20^{\circ}\text{C}/\text{h}$.

Isothermal period is a key area in the heating cycle. Once the temperature in the concrete reaches the required maximum, from that point, the temperature needs to be maintained so that curing can occur efficiently. The idea of electric heating is to not keep on increasing the internal temperature of the cementitious material but to maintain it at a steady state by included the dissipation of heat and other losses. The dissipation of heat depends on the surface moduli of the specimen which in turn depends on the geometry and the size of the specimen used. It can be expected that concrete can retain the heat that is generated in the heating phase so sudden spikes of current for a shorter time interval is also enough to maintain the temperature within the recommended range of internal temperatures. Through various research, it has been found that the maximum internal temperature of the concrete should not exceed 80°C and that the optimum range is between 60°C and 80°C [16][41].

The cooling phase is useful if the specimens are adequately insulated to retain the heat for quite some time before they are exposed to the environment. Though not part of the heating cycle,

care should be taken to avoid rapid cooling of the specimen during and after the isothermal cycle ends [16][41].

2.10 Effects of Electric Curing on Concrete Properties

2.10.1 Compressive Strength

The primary motivation for using accelerated curing methods is to achieve a higher early-age compressive strength of the concrete element, and increasing curing temperatures increase early strength development [28] [13][40][34][9][44][6]. Though elements cured by electric curing have higher early-age compressive strengths are higher than elements cured under standard temperature conditions, there is quite some scattering in the results concerning the 28-day compressive strengths. The 28-day compressive strength depends on the current regime. A higher current regime (in terms of intensity and length of curing) might not necessarily have the highest 28-day compressive strength. At the same time, the samples subjected to a lower current regime need not have the lowest compressive strengths [13][40][34].

2.10.2 Setting Time

Uygunoğlu, T. et al. [40] reported a decrease in setting time with increasing voltage intensities. The heat generated due to the passing current would enhance the hydration resulting in the formation of solid products, which in turn harden the mix. The temperature peak coincides with the point (time) when the final set occurs [40].

2.10.3 Porosity

Bajza A.et al. [3] compared heat-treated samples with control samples (cured under standard conditions) and reported that the increase in the intensity of the heat applied to the specimen results in a coarser microstructure. Kjellsen, K. O.et al. [17] reported that the higher the curing temperature, the higher the volume of total porosity and larger pores in a specimen. A higher volume of large pores makes the specimen more prone to the permeation of contaminants such as chlorides, causing durability issues. Applying heat for curing reduces the diffusion of the individual cement particles and results in the non-uniform distribution of hydration products within the matrix. These render the samples more coarse microstructure than moist cured samples. The uneven distribution of hydration products and the specimen's increased porosity are not suitable for the durability performance of concrete [9].

2.10.4 Ettringite Formation

Though not an immediate outcome of accelerated heat curing techniques, this is becoming a point of study in recent years. The ettringite formed during the initial hydration of cement gets broken down into sulphate and aluminate ions due to applications of higher levels of heat for curing. Over time, moisture penetration into the concrete specimens results in delayed ettringite formation. By this time, the cementitious specimen has a packed microstructure and higher strength, and the formation of new products can not be accommodated as it would require space. Delayed

ettringite formation combined with alkali-silica reactions, freeze and thaw, causes durability issues [9][47].

2.11 Summary and Outlook of Literature Study

In this chapter, curing at elevated temperatures and a brief about a few accelerated curing methods have been presented. The main focus of the literature study is to give a detailed insight into electric curing and its working mechanism with respect to the electrical properties of concrete, the conventional curing cycle, and the effect it has on the material properties of concrete. Electric curing has both positive and negative side effects, where increased early-age compressive strength and acceleration of the hydration process add to the former, while increased porosity, decreased long-term strength, and delayed ettringite formation add to the latter. Along with electric curing, the mechanism of cement hydration with time and the effects of admixtures on concrete mixes have also been briefly discussed. The literature study also reports assessing the setting time of samples undergoing electric curing with temperature evolution.

The application of current to fresh concrete, surpassing the pre-heating storage period, and its effects on concrete samples require a detailed review. Depending on the outcomes of the current study, the usage of current to alter setting time can be discussed. For this purpose, the following areas have been investigated:

- Setting up of an electrical curing setup which accommodates direct current, alternating current and pulsed direct current
- Experimental tests to assess the setting time of cement mortar subjected to electrical treatment with direct current or alternating current or pulsed direct current
- Experimental methodology to quantify the compressive strength and resistivity of cement mortar samples subjected to electrical treatment
- Study the correlation of setting time with experimental data, such as temperature evolution during the curing period.

The aspects mentioned above are dealt with in the subsequent chapters.

3 Experimental Study

3.1 Outline of the Experimental Study

This chapter covers aspects of the properties of the materials used in this research and the methodology adopted to prepare the samples used as both control and electrically cured specimens and to assemble the setup for curing. The test setup and its functioning when the samples are subjected to different currents and curing regimes are described.

3.2 Sample Preparation

The mix used for this research is similar to the one used in studying the effects of stray current on hardened cement mortar samples [34]. For this purpose, CEM-I (42.5N) cement (Table 1) was chosen with a cement: sand ratio of 1:3 and a water-cement ratio of 0.5 was adopted.

Chemical Compound	Percentage (%)
CaO	63.9
SiO ₂	20.6
Al ₂ O ₃	5.01
Fe ₂ O ₃	3.25
SO ₃	2.68
K ₂ O	0.65
Na ₂ O	0.3

Table 1: CEM-I-42.5N - Chemical Composition

The particle size distribution of the fine aggregates are as follows:

Particle size	Weight percentage (%)
2mm-1mm	33
1mm-0.5mm	34
0.5mm-0.25mm	21
0.25mm-0.1mm	12

Table 2: Particle size distribution of fine aggregates

The samples that were cast were 40x40x40 mm³ mortar samples. The samples were cast in silicon moulds in order to accommodate the Ti-MMO meshes (Figure 2) that are to be placed in the sides of the mould to act as electrodes for application of current through the samples.



Figure 2: Ti-MMO Mesh



Figure 3: Mould setup for the setting time test

Figure 4 shows a cube sample that is electrically cured.



Figure 4: Cube specimen subjected to electric curing

Materials	Weight (grams)
Cement	357.26
Fine aggregates	1071.78
Water	178.63

Table 3: Material weight

Fine aggregate size distribution	Weight in grams
2mm-1mm	353.68
1mm-0.5mm	364.40
0.5mm-0.25mm	225.07
0.25mm-0.1mm	128.61

Table 4: Fine aggregate weight distribution

Mixing was done using a Hobart mixer. First, the aggregates were put in the mixer for about 30 seconds to get a homogeneous mix of the aggregates as they were separately weight-batched. The mixer was stopped, and the cement was added to the aggregates. After 2 seconds of mixing the aggregates and cement, half the quantity of water weighed was added to the mixture of

aggregates and cement. This time is noted down as T₀, later used to estimate the setting time. Mixing is done for an additional 2.5 mins, and the rest of the water is added. When an accelerator* is used, it is mixed with the second half of the water and added after 2.5 mins. In entirety, mixing was done for 4 mins, which was maintained for the preparation of all samples.

*(The accelerator, CUGLA-HA-20, used is a chloride-free hardening accelerator whose effective ingredient is nitrates. The accelerator comes with a 50% concentration. The accelerator was mixed with the mixing water while adding it to the cement mortar. The maximum recommended use is 3% relative to the cement content used. The minimum percentage, as per product specifications, is 0.2%.)

For our experiments, the mean value of 1.6% and a maximum value of 3% is chosen for addition to the mixture. The conventional setting time, frustum mould, was not used for the setting time test. Instead, the cube mould was used for the compression testing purpose was used. The standard vicat is frustum shaped to allow the mixture to flow and settle. In the standard test, the mixture is compacted by hand after it is poured. The flow and compaction by hand are not possible when the cube mould is used. The flow is restricted because of the geometry of the mould, and compaction by hand is not advisable as it would displace the electrodes. To account for the restricted flow and compaction, after pouring the mix, the moulds are compacted for a short duration of 3 seconds on a vibrating table.

The samples to be electrically cured are subjected to curing exactly after 15mins after adding water to the mix to maintain uniformity while noting the setting time readings. The specimens are subjected to electric current for 6 hours. A 6-hour curing cycle was chosen as the setting time for the CEM-I cement mortar takes roughly 6 hours measured using the standard Vicat (conventional mould) and the Modified Vicat (box mould in figure 3).

Also, considering shifts in the prefab industries, which should be 6-8 hours [41], a 6-hour curing period would be a wise choice when we look at the industrial application.

3.3 Curing Setup

The different types of currents are generated with different power sources and with a few additional components, which will be addressed in the subsequent pages. The main components of a curing setup are shown below:

1. **Power Supply Unit (PSU) 1** Variable power supply, 0 - 32 V DC, 0 - 2 A
2. **Power Supply Unit (PSU) 2** Fixed power supply, 15 V DC, 2 A
3. **Switching Box** High-speed MOSFET switch with current and voltage sensors, 1.5 kHz
4. **Variac** Variable Transformer, 0 - 230 V AC, 50 Hz
5. **Transformer Box** Fixed Transformer, 230 V AC → 80 V AC, 50 Hz
6. **Current Control Printed Circuit Board (PCB)** Resistance-based current control board
7. **Analog to Digital Converter (ADC) Box** Converter to feed all analog signals into the computer

8. **Thermocouples** Type K thermocouple, -40 - 1100 °C, Nickel Chromium/Nickel Aluminium, stainless steel sheath
9. **Electrodes** Titanium mixed metal oxide meshes

The setup for conventional electric curing (AC) [13] consists of:

- (a) Power Supply
- (b) Transformer
- (c) Variac
- (d) Electrodes
- (e) Samples

The power supply is alternating current - the conventional output we get from our daily power sockets. But this power source has a voltage of 240V at a frequency of 50Hz. This voltage needs to be stepped down to regulate the voltage across the sample. The former is done with the help of a transformer and the latter by a Variac. To measure the voltage, current and power, a voltmeter, ammeter and wattmeter are connected across and in series, respectively. The electrodes usually used are steel plates attached to the sample sides, and the voltage required is applied across the samples [13].

Setup for curing in this research: For this research, both direct current and alternating current are applied across the samples to find if they can accelerate the setting of the samples and also to analyse other material properties. A few changes from the conventional method are brought about to accommodate the usage of both types of current.

1. There is no physical voltmeter, ammeter or wattmeter. All the readings are taken with the help of a PCB and a computer.
2. The electrodes used here are Ti MMO meshes and not plates.
3. In most electric curing setups, the samples are not secluded from the environment. Since we are measuring the setting time by applying electric current, the heat generated is used as much as possible by placing the samples in a Styrofoam box. The sample isolation helps us know how the heating of the sample accelerates the setting time.

3.3.1 Direct Current

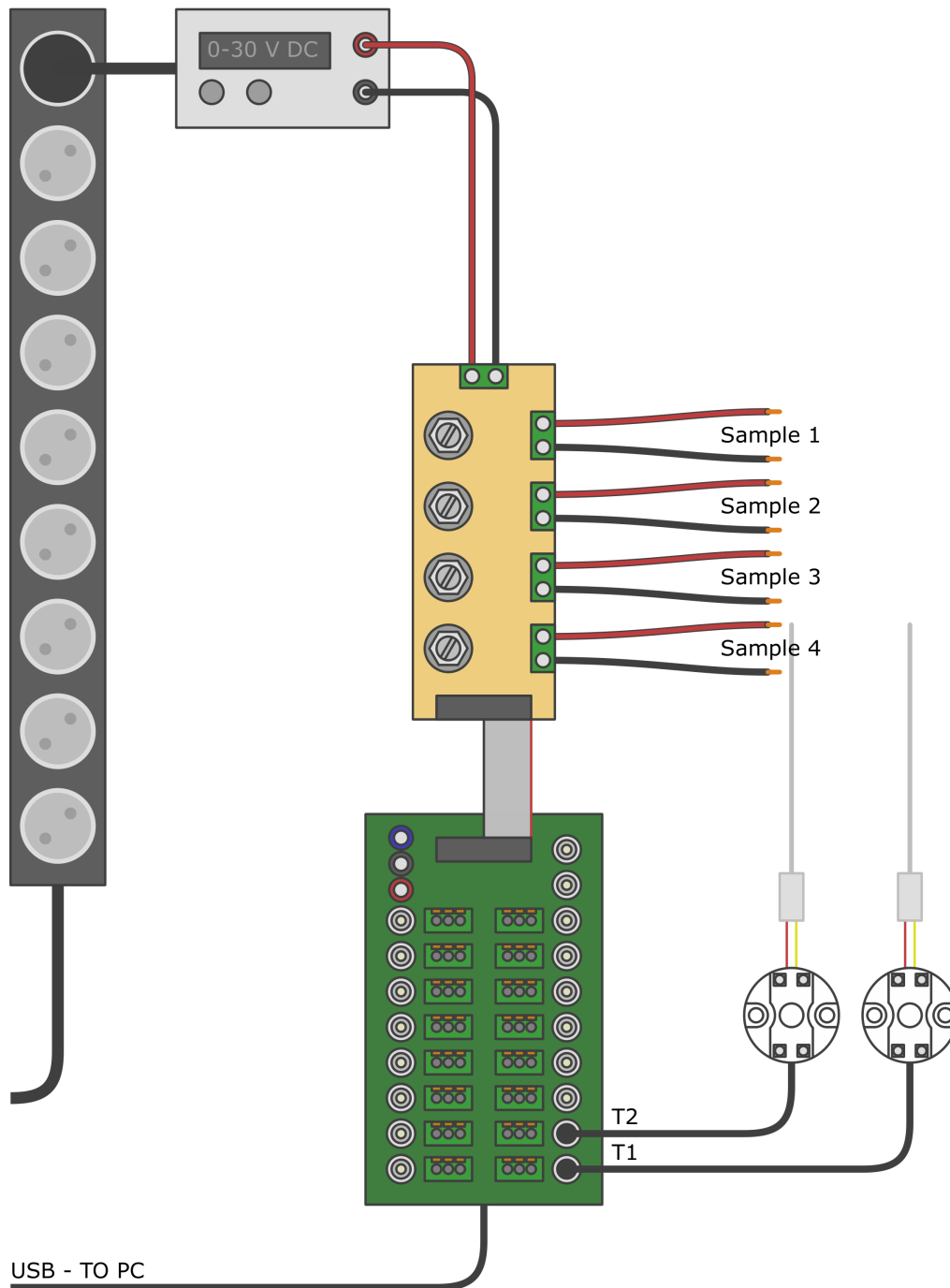


Figure 5: Direct current curing setup

In figure 5 the power supply is a current-controlled direct current supply source. A constant current source is used to have constant current density across the sample. If, in this case, a voltage control source is used, then the voltage required to have the same current density would increase with the increase in resistance, in other words, with an increase in time.

The electrodes are Ti-MMO meshes and not steel plates since the current densities we have chosen (Table 5) would result in the corrosion of the steel plates. Steel would have been a choice if the current had to be applied for a shorter time or if the current intensity was low. But the current application period is 6 hours, and hence there is a chance that corrosion might occur. Titanium mesh is used as electrodes to avoid the possibility of corrosion and debonding.

The DC power supply was connected to the current control PCB; from there, it is connected to the USB ADC and then to the computer with the recording software.

Table 5 shows the DC regimes adopted for the curing cycles

Current Density (A/m ²)	Current (mA)*
5	8
10	16
20	32

Table 5: Direct current regimes

[*Note: Since the sample has a cross section of 40mm x 40mm, the current that needs to be applied across the sample is obtained by multiplying the current density and the area of cross section of the sample ($A=0.0016\text{m}^2$). Also, $1\text{A}=1000\text{mA}$]

These current regimes were chosen to keep in mind the current densities that can be applied and replicate the regimes used for cathodic protection, especially in the initial stages of the cathodic protection regime [5].

3.3.2 Alternating Current

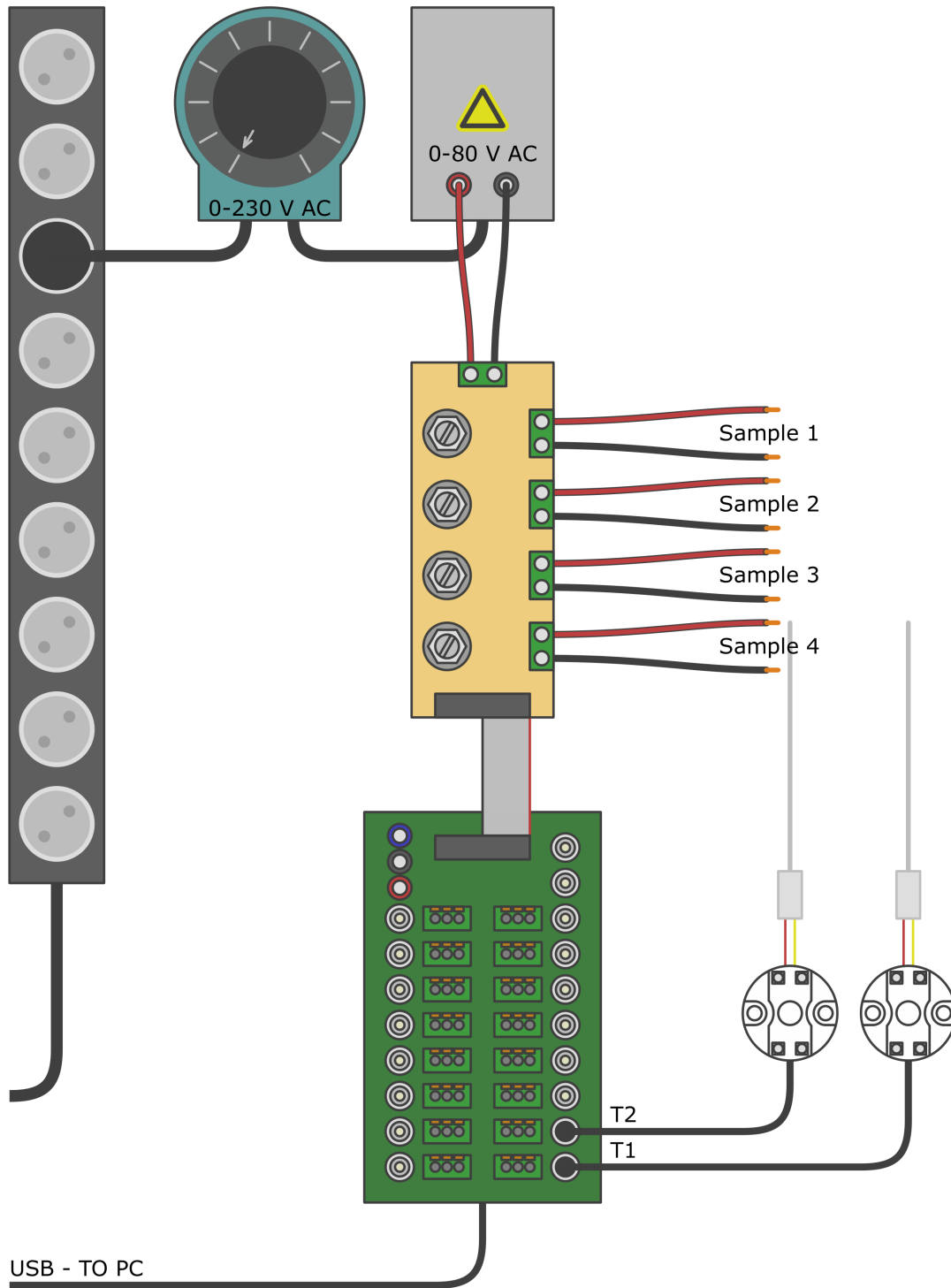


Figure 6: Alternating current curing setup

Figure 6 shows the curing setup that uses alternating current. The alternating current setup (Figure 6) is similar to the conventional setup (Power source → Variac → Transformer → Samples) [13]. In the existing setup, input voltage, current, and voltage across the samples are taken with the help of a PCB and software. A transformer is used to step down the voltage from the power source, and a Variac is used to regulate the voltage. The software records the reading, but voltage regulation is made manually.

The electrodes used here are also Ti-Mesh. In this case, steel plates could have also been used as the chances of corrosion due to alternating current are less than the DC regime. But, to maintain uniformity across the experiments, the electrodes were not changed.

A set of voltage regimes was chosen to be kept constant throughout the 6 hours of treatment period are shown in Table 6.

Voltage (V)*
5
10
15

Table 6: Alternating current regimes

3.3.3 Pulsed DC

Pulsed Direct current was chosen to reduce direct current effects on the sample (hydrogen generation, polarisation). Both DC and pulse DC is not generally used for curing. Since the effect it has on the setting is a key area of the research, pulse DC is not a regularly used current type in the civil industry. The curing setup had to be updated compared to the above setups for the direct and alternating currents, as shown in Figure 7

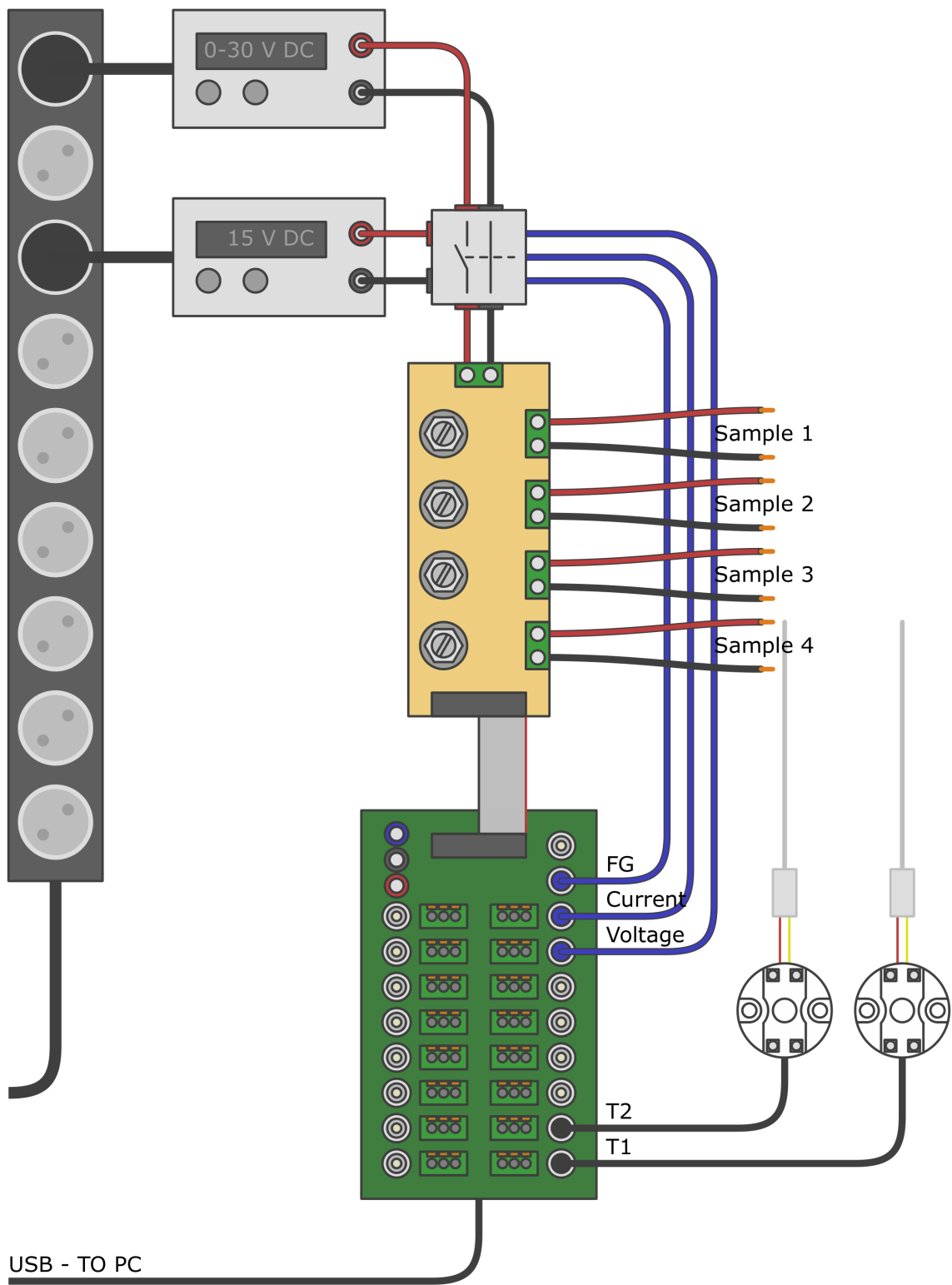


Figure 7: Flowchart of Pulsed direct current curing setup

In Figure 7, the power supply unit is a direct current supply unit, and the power supply is connected to a switch box. This switch box makes it possible to disconnect the circuit for a short time to generate the pulse. Since the chosen frequency is high (1500Hz) for regular switches, a special switch was chosen. This switch needs to be powered by a 15V source to function. So the power supply unit is connected to the switch box, which is connected to the Current PCB to supply current for the samples. The current PCB and USB PCB are connected so the software can record the current and voltage intensities of the pulse generated along with recording the current and voltage across samples.

The current regime chosen is similar to the direct current regimes to bring about a common comparison point between the two types of current and is shown in Table 7

Current Density (A/m ²)	Current (mA)*
5	8
10	16
20	32

Table 7: Pulsed Direct Current regimes

The frequency determines the pulse duration, and how long the pulse acts on the sample is determined by the duty cycle. The duty cycle is the ratio of time when the circuit is loaded, i.e., ON, to the time of one cycle, i.e., OFF+ON). In our case, the duty cycle chosen is 25%.

Since the frequency is 1500Hz, the duration of one pulse is $f = \frac{1}{T}$ where T is the time period, so the time period in our case is $T = \frac{1}{f} = \frac{1}{1500} = 0.666ms$. With a duty cycle of 25%, the duration for which the current is on i.e., the duration for which the current is acting on the sample is 25% of the time period.

$$T_{on} = 0.25 * 0.666 = 0.166ms \quad (3.1)$$

3.4 Behaviour of Voltage and Current

3.4.1 Direct Current

The current and voltage trend of 16 mA current i.e., 10 A/m² is shown in Figure 8.

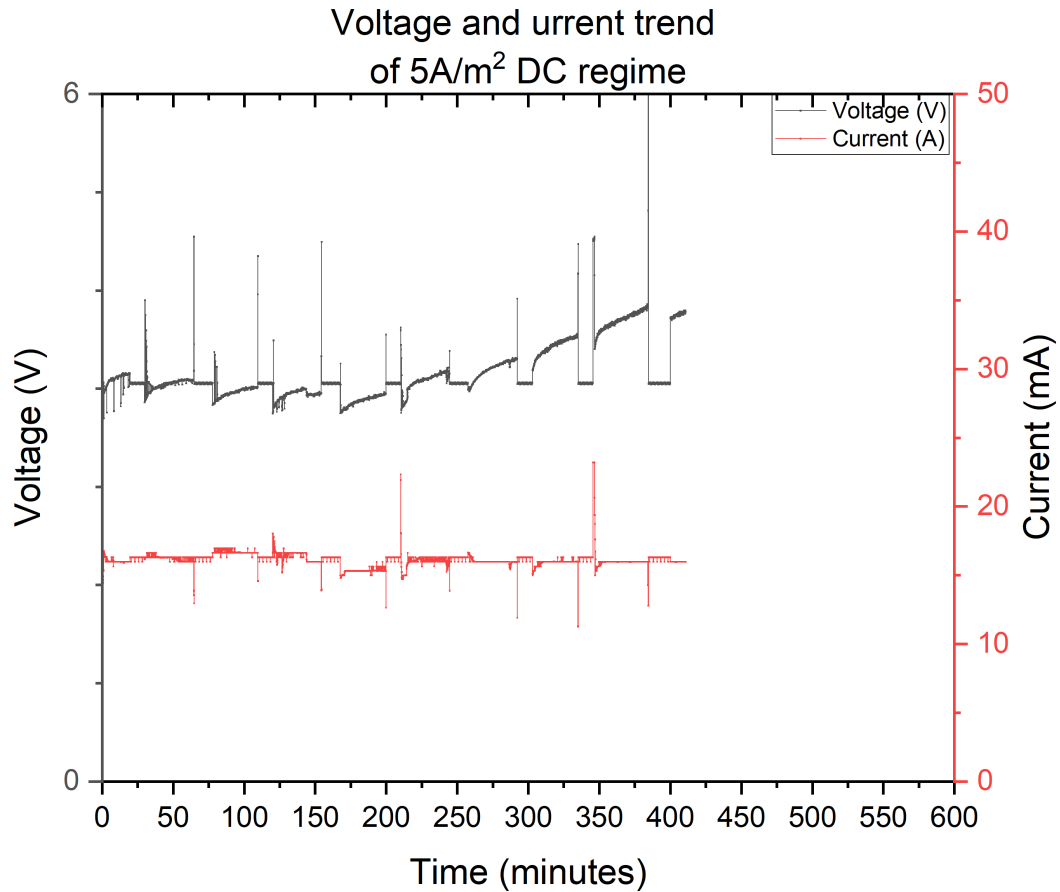


Figure 8: Voltage and current trend for 10A/m²

The behaviour of the 5 A/m² and 20 A/m² voltage and current is similar with obvious changes in magnitude, are also subject to voltage and current fluctuations.

In Figure 8, the current and the voltage are subject to fluctuations throughout the application of current till the setting time occurs. The fluctuations are present as the current is controlled manually and once the current is set with the resistors on the current PCB, it takes a few seconds to stabilise and hence, the minute disturbances or noise.

3.4.2 Alternating Current

The current and voltage trends for the 10V regime is shown in Figure 9.

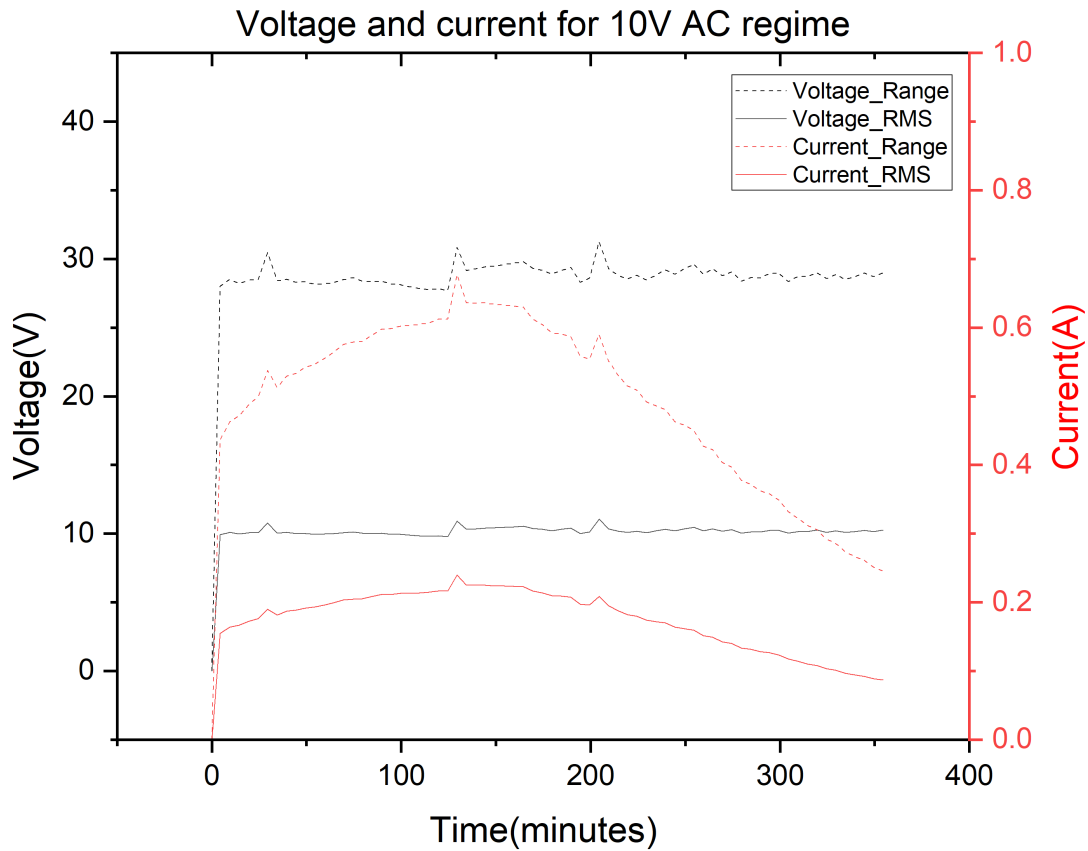


Figure 9: Voltage and current trend for 10V

The measurements recorded are the range values (i.e., peak to peak values of the voltage/current wave) which is given by VRANGE and IRANGE respectively. In order to calculate the voltage, we need to take the Root Mean Square value (RMS), VRMS. To calculate this value, we take a value from range (Vrange) and put it in the equation shown below:

$$V_{RMS} = V_{range} * 0.5 * 0.707 \quad (3.2)$$

The factor 0.707 is a factor that is used to find out the mean of the sine wave (Literature) This conversion is also applied to current.

$$I_{RMS} = I_{range} * 0.5 * 0.707 \quad (3.3)$$

The voltage and the current trends are similar for the other two regimes except for the changes in magnitude and fluctuations or noise. We can see that the current increases, reaches a peak value, and decreases as time increases. With the hardening of the mortar, the voltage applied across the sample no longer generates the same current as it did earlier, i.e., with an increase in resistance, the current reduces for the given constant value of voltage.

3.4.3 Pulsed Direct Current

The voltage and the current graphs are shown in Figure 10, for the $10A/m^2$ pDC regime:

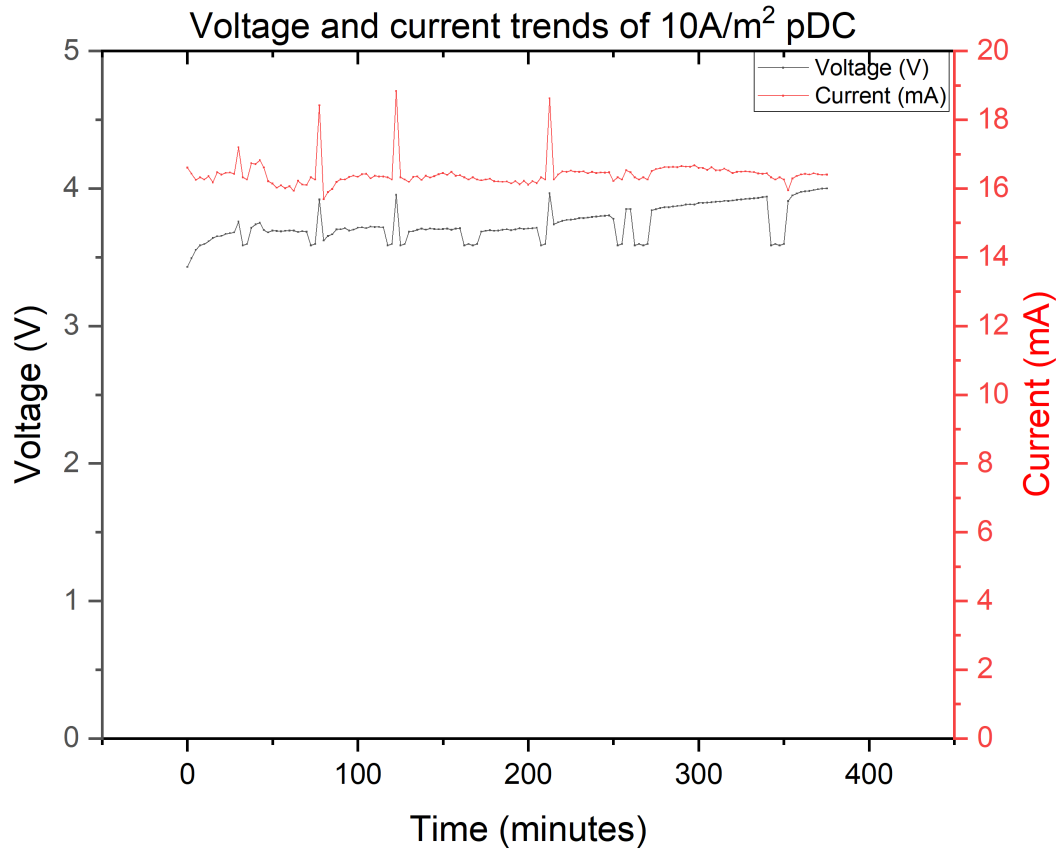


Figure 10: Voltage and current trend for $10A/m^2$ pulsed direct current

From Figure 10, the voltage and the current behaves similarly to how both would behave in the case of the $10A/m^2$ direct current regime. In Figure 11, we can see the pulse behaviour of voltage and current.

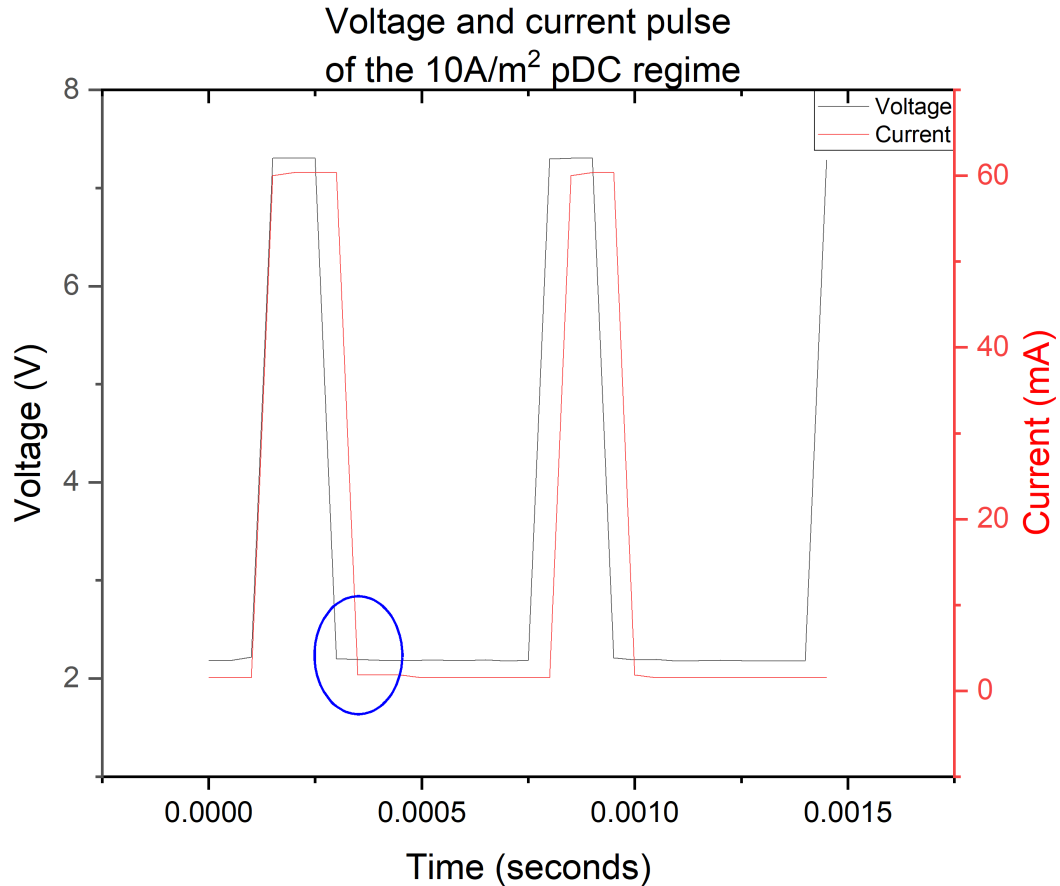


Figure 11: Voltage and current trend for $10A/m^2$ pulsed direct current

You can see that the current scale shows a peak value of 65mA, and then the pulse drops to almost zero. When we take the mean values from the pulse for one second, we get 16mA. This is how a pulse works, i.e., if we take one second and consider the duty cycle of 25%, the load on the circuit is ON (and subsequently the voltage) for 25% of 1 second and OFF for the rest 75% of one second.

We can see in Figure 11 (circled) that even when there is no current, there is a voltage value, but this is not possible, and the 'lag' in the voltage is because of the measurement card used to take the reading from the USB PCB and send it to the PC. The measurement card uses multiplex channelling. A multiplexing channel means there are 5 channels from which readings must be taken. The card moves from one channel to another in sequential order. Since, in our case, the sampling rate (the number of values noted per channel) and the total number of channels are high, generating the values on the graphs is delayed.

4 Testing Specimens

4.1 Outline

This chapter discusses the methodology adopted for the experimental work and the working of the equipment used to collect data.

4.2 Setting Time

According to EN-196-3-2016 [27], the principle of the setting time test is "The setting time is determined by observing the penetration of a needle into a cement paste of standard consistency until it reaches a specified value". Since a modified vicat setup is adopted in this research, referencing had to be done to justify why and if the modified Vicat would have a reliable output. The Manual vicat apparatus that was used for this study is shown in Figure 12:

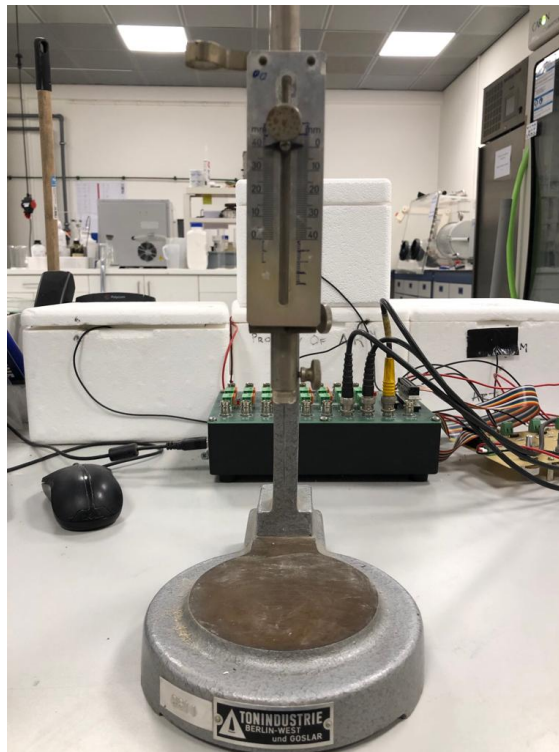


Figure 12: Voltage and current trend for $10A/m^2$ pulsed direct current

In this study, the setting time of mortar is tested. For this, the mixture is prepared as mentioned in the sample preparation. The cement, aggregates and water are measured to an accuracy of (\pm)1 g using a balance and are mixed using the HOBART mixer. Before mixing, the mould with the base plate is used to calibrate the vicat apparatus so that the penetration readings are mostly accurate. After the calibration, the mixing procedure is started (Refer to appendix A).

4.3 Modified Vicat

Changes were made to the conventional vicat apparatus, and the accuracy of the results was verified by using the conventional vicat test as a reference point.

The following were the changes:

1. The mould being a frustum, is not used as the current lines were not expected to be uniform as we would expect in a rectangular mould. This conventional mould has an open-ended base, so the attachment of the electrodes is not possible. So, the mould chosen was the rectangular mould used for casting cubes for the cube-compression test. This cube mould also neglects the differences (if there were any) between the samples tested for compression and the samples used for setting.

According to EN-196-3-2016, the mould that can be used should be of depth 40mm and should be referenced with the conventional method.

The standard frustum mould would allow space for the flow of the mortar, and minimal compaction is sufficient. However, for the box mould, compaction had to be done on a vibrating table: (i) to allow levelling of the mortar, (ii) to avoid clumping of the mortar on the top, (iii) box mould having confined space would not allow the mortar to flow into the mould given the consistency of our mix. Figures 13 and 22 show the box mould with a non-porous glass plate with and without electrodes respectively.



Figure 13: Box mould without electrodes



Figure 14: Box mould with electrodes

2. Data points – The data points in a conventional test would be around 23 (for the time interval and the mix that we have chosen for the conventional test); since a smaller surface area is available for obtaining the data points, there is a possibility to take only 9 (45min time interval) readings. The reproducibility of the results can be ensured by increasing the number of setting time trials with the box mould. Another essential aspect would be first comparing the results of the conventional and modified tests to see how much the results vary between the two moulds. The comparisons were made, and deviations were such that results were almost similar between the conventional and modified methods.
3. When setting would not occur under specific current regimes, the interval between the last 3 points was changed to 90mins (from the chosen 45 minutes). The mould depth of 40 (\pm)3 mm was assured by placing a base plate made of glass at the bottom of the mould to replicate the non-porous base in the conventional method. The effective height was checked to be 40mm while the calibration was done to ensure the accuracy of the results.

The sample preparation (weighing, mixing) is similar to what was adopted in the conventional tests. The only inclusion was that of the vibration for 3 seconds. Before the readings are taken, the vicat apparatus must be calibrated according to the mould and the base plate used.

For both conventional and modified setting time tests, the sample was stored in a styrofoam box for seclusion from the environmental factors as much as possible. It was done to minimise the loss of heat generated during the curing process.

4.4 Compression Test (1D, 3D and 7D)

The compression test is done on 40x40x40mm cubes similar to the ones used for the setting time test and was carried out using an automated compression testing machine. The rate of loading chosen was 1kN/s, and the start load was 100kN. The electrically cured and reference samples were tested at 1,3, and 7 days to study the early age compressive strength. The electrically cured sample was kept in a temperature and humidity-controlled room after being subjected to the curing cycle of 6 hours, with reference samples being kept in the curing room after de-moulding them at the end of one day and were later tested for 3- and 7-day strengths.

4.5 Resistivity Measurement

The electrical resistivity of the cube samples, electrically cured and reference, were taken throughout the setting of the samples. The resistivity measurements were done through a 2-pin method (pins here refer to the Ti- MMO electrodes). An alternating current source of 1mA and 250Hz was used along with a multimeter to measure the voltage reading of the sample. The resulting voltage measurement obtained can then be translated to finding the resistance and, subsequently, the resistivity of the sample using the formula:

$\rho = R * \frac{A}{l}$, where R is the resistance at that particular instance which is given by $R = \frac{V}{I}$, $V \rightarrow$ voltage(V), $I \rightarrow$ current(A), A is the area of cross-section of the sample (Here $A = 0.0016m^2$), l is the length of the sample ($l = 0.04mm$)

5 Results

5.1 Overview of results

The setting times of each electrically treated and control sample have been represented in graphs and tabulated at the end of each current regime type (DC, AC and pDC). Following the setting time results, the compressive strengths of electrically treated and control samples for one day, three days and seven days have been represented in graphs. Three cubes were cast for the compressive strength test, and the average values of their compressive strengths were taken to represent the results. The effect of accelerators and electric treatment with the 15V AC regime is also investigated.

Resistivity readings, along with the setting time curves, have been presented as graphs. The temperature of the samples was measured using isolated thermocouples and has been represented. The voltage and current values were recorded in a computer through a USB print control board (PCB). Electrical data such as charges, power, and energy were calculated with these values.

5.2 Setting Times

5.2.1 Direct Current Setting Times

In this section, the setting times of mortar subjected to $5A/m^2$, $10A/m^2$ and $20A/m^2$ DC regimes are represented in Figure 15. An overview of these results is presented in Table 8. The DC setting times are compared with the setting time of the control specimen, where the control specimen is allowed to set without the application of current.

Table 8 gives a summary of the setting times obtained from the modified vicat test for the different DC regimes

Regime	Initial setting time (mins)	Final setting time (mins)
Vicat (Control)	165	360
Box (Control)	170	405
05 A/m ²	202	405
10 A/m ²	145	405
20 A/m ²	138	405

Table 8: Setting times obtained from modified Vicat apparatus testing for the DC regimes

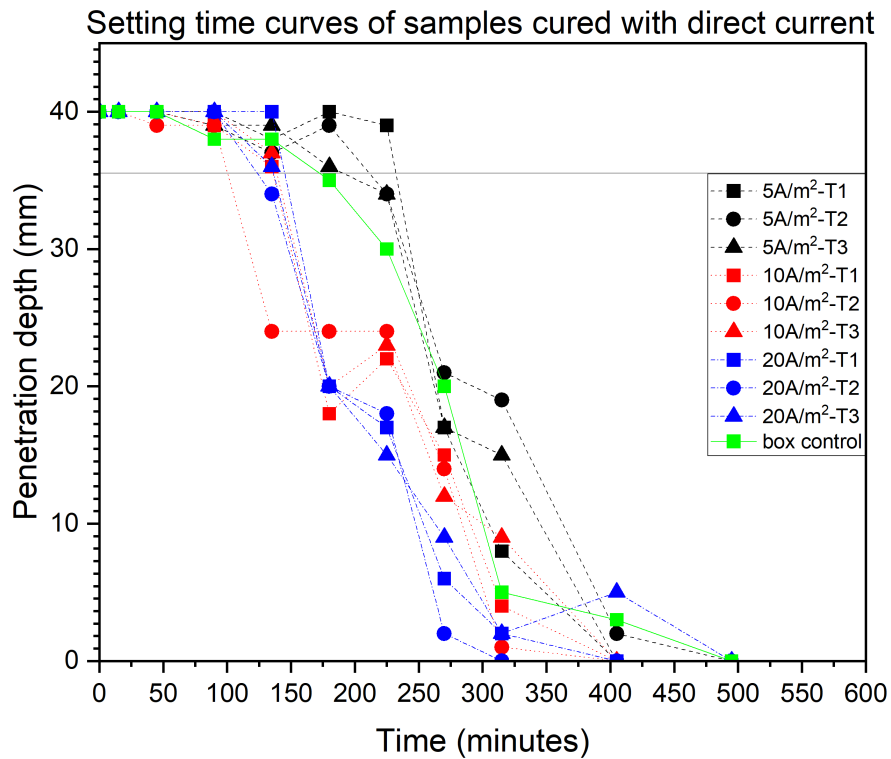


Figure 15: Setting time curves of samples subjected to direct current regimes

From figure 15 and Table 8, the influence of direct current on setting time is visible compared to the control curve. In figure 15, a reference line of $y=35$ is provided and is used for graphically obtaining the initial setting time from the setting time curves i.e., the intersection between the $y=35$ and the setting time curve is projected to the x-axis, and this x-intercept value is taken as the initial setting time. T1, T2 and T3 in Figure 15 refer to the setting time trials 1, 2 and 3 respectively under this case. Box control is the curve that gives the setting time curve of mortar subjected to no current. The initial and final setting times for the mortar using the conventional vicat mould are 165 minutes and 360 minutes, respectively. The initial and final setting time of the mortar using the box mould is 170 minutes (3 sample average) and 405 minutes, respectively. There is a difference between the setting times for the mortar in different moulds. The initial and final setting time of the box mould has an overestimation of 9% and 12% respectively when compared to the conventional vicat mould. The setting time curves of 10 A/m² and 20 A/m² show that the rate of setting is significant when compared to the control curves. But, this does not hold true for the 05 A/m² setting time curves. The initial setting times obtained from the curves for the 05 A/m², 10 A/m², 20 A/m² regimes are 202, 145, 138 minutes respectively while the final setting times were 405 minutes for all the samples cured with DC regimes.

5.2.2 Alternating Current Setting Times

This section consists of the setting times of mortars subjected to alternating current regimes of 5V, 10V and 15V, respectively, as represented in Figure 16. A summary of the initial and the final setting times is presented in Table 11.

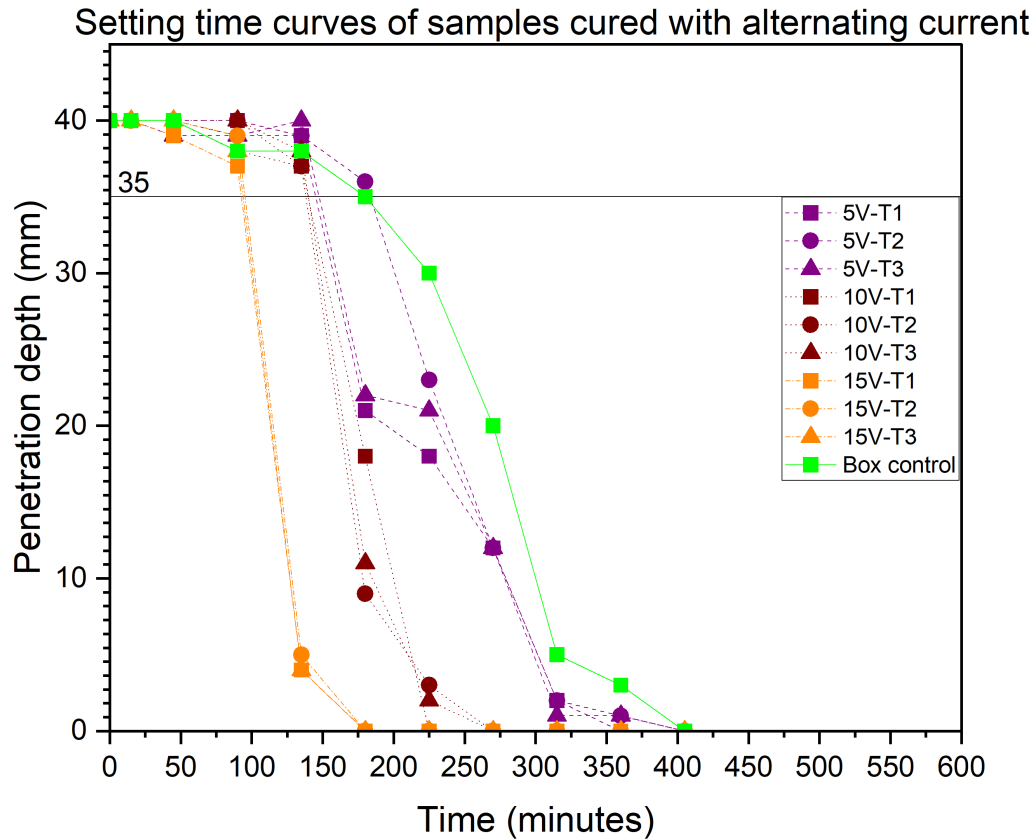


Figure 16: Setting time curves of samples subjected to alternating current regimes

Table 9 gives an overview of the setting times of the respective current regimes.

Regime	Initial setting time (mins)	Final setting time (mins)
Box (Control)	180	405
5V	162	405
10V	139	270
15V	94	180

Table 9: Setting times obtained through modified vicat apparatus for AC regimes AC regimes

In Figure 16, a reference line of $y=35$ is provided and is used for graphically estimating the initial setting time from the setting time curves i.e., the intersection between the $y=35$ and the setting

time curve is projected to the x-axis, and this x-intercept value is taken as the initial setting time. T1, T2 and T3 in Figure 16 refer to the setting time trials 1, 2 and 3 respectively under this case. Box control is the curve that gives the setting time curve of mortar subjected to no current. Figure 16 and Table 11 show a clear difference in the final setting times of mortar with increasing voltage intensity. The average initial and final setting time for the 5V regime is 162 minutes and 405 minutes, respectively; for the 10V regime, it is 139 minutes and 270 minutes; for the 15V regime, it is 94 minutes and 180 minutes, respectively. Comparing the 15V electrically cured specimen, which show a drastic reduction in setting time, and control setting times from figure 16 and Table 11, the initial and final setting times are decreased by 47.2% and 55.5%, respectively. The initial setting time of the sample subjected to the 5V regime decreases by 10% compared to the control specimen and there is no difference in the final setting time. Comparing the 10V specimens and the control, the initial setting time is decreased by 22.7% while the final setting time is decreased by 33.3%. This decrease could be due to the temperature evolved due to the intensity of voltage applied across the sample.

5.2.3 Alternating Current- 15V (Accelerator) Setting Times

The setting time of mortar with different accelerator percentages subjected to a 15V alternating current regime is presented in Figure 17 and Table 10.

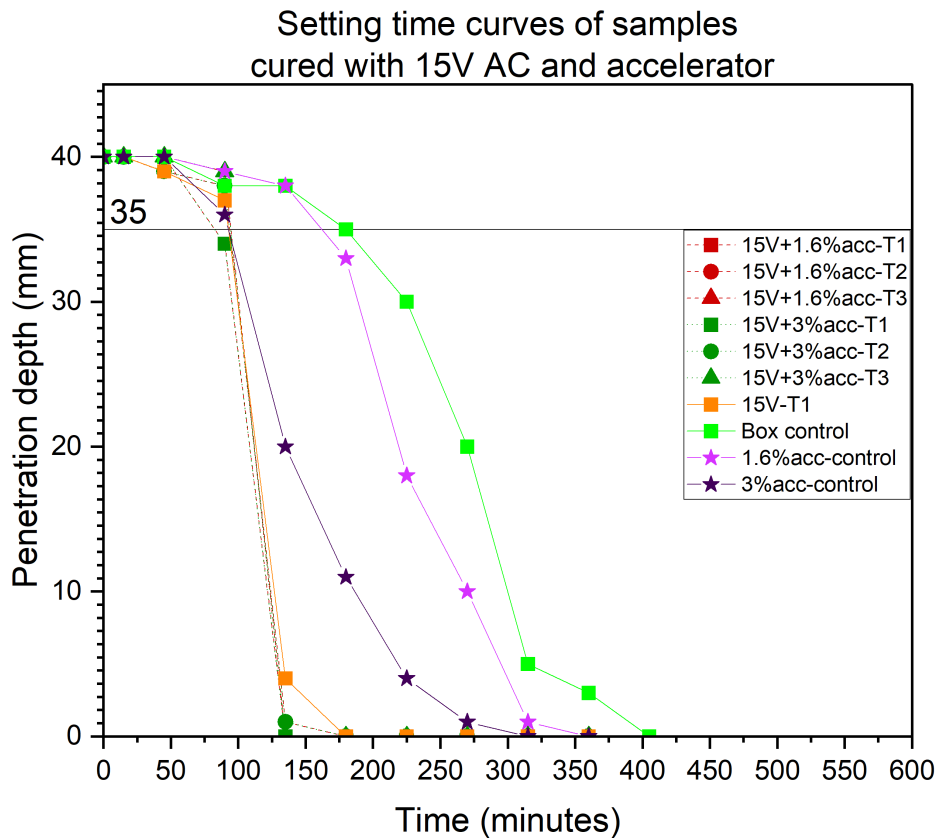


Figure 17: Setting time of cement mortar with chemical accelerator subjected to 15V AC

Table 10 gives an overview of the setting time of mortar with accelerators subjected to 15V AC.

Accelerator concentration	Initial setting time (mins)	Final setting time (mins)
1.6%-15V	90	135
3%-15V	90	135
1.6%-control	160	315
3%-control	110	270
15V-control	94	180
Box control	180	405

Table 10: Setting times obtained through modified vicat apparatus for AC+accelerator

In Figure 17, a reference line of $y=35$ is provided and is used for estimating the initial setting time from the setting time curves i.e., the intersection between the $y=35$ and the setting time curve is projected to the x-axis, and this x-intercept value is taken as the initial setting time. T1, T2 and T3 in Figure 17 refer to the setting time trials 1, 2 and 3 respectively under this case. Box control is the curve that gives the setting time curve of mortar subjected to no current. From Figure 17 and Table 10, the decrease in the setting time as a result of combining an accelerator and current is visible. The initial and final settings of specimens subjected to 15V and accelerators (both 1.6% and 3%) are 90 minutes and 135 minutes, respectively. The control specimens with accelerator percentages of 1.6% and 3% have initial setting times of 160 and 110 minutes and final setting times of 315 and 270 minutes respectively. On comparing with the setting times of the 15V AC regime without the accelerator, both mortars with accelerators show reduced initial and final setting times. The decrease in initial and final setting time could be because of the accelerator and the influence of the voltage across the sample, respectively. There is a 33.3% decrease in initial setting time when the accelerator is used when compared with the box control specimen (without current and accelerator).

5.2.4 Pulsed Direct Current Setting Times

The setting times of mortar subjected to the pulsed direct current regimes of $5A/m^2$, $10A/m^2$ and $20A/m^2$ are represented in Figure 18. An overview of the setting times is presented in Table 12.

Table 11 gives a summary of the setting times presented in figure 18.

Regime	Initial setting time (mins)	Final setting time (mins)
5 A/m ²	170	450
10 A/m ²	153	450
20 A/m ²	144	495

Table 11: Setting times obtained from modified vicat apparatus for pDC regimes

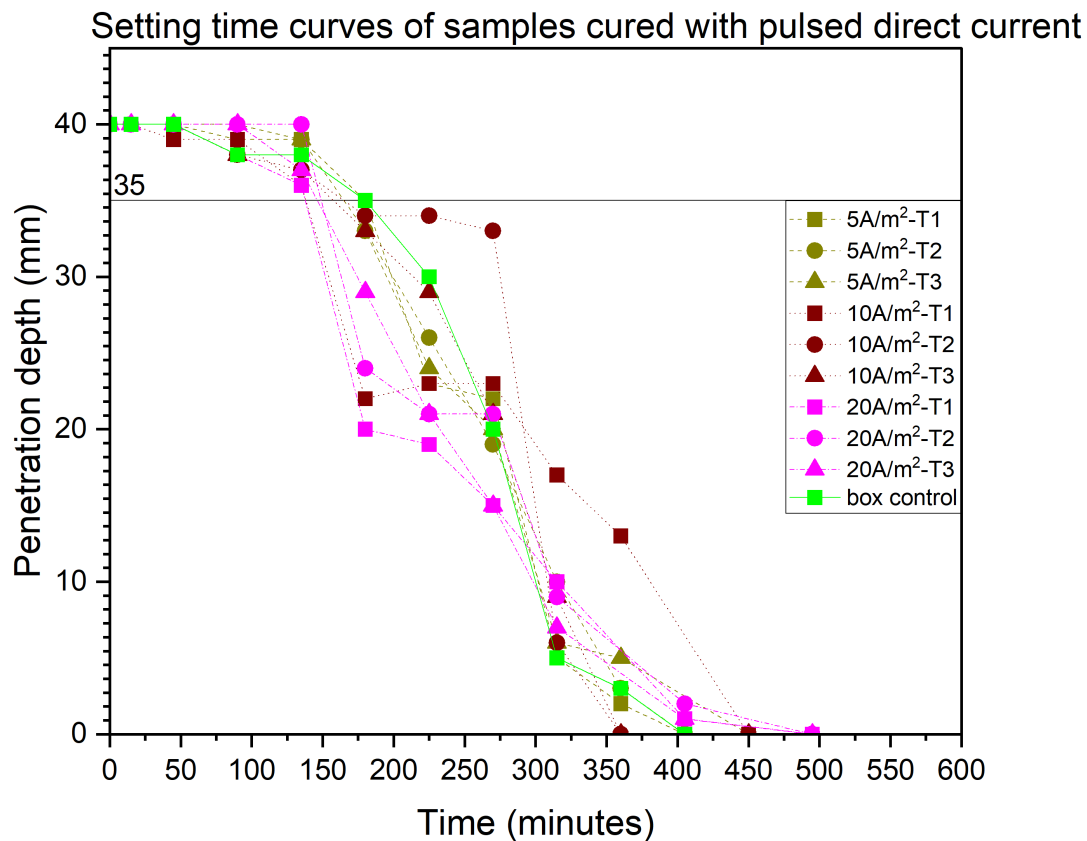


Figure 18: Setting time curves of samples subjected to pulsed direct current regimes

In Figure 18, a reference line of $y=35$ is provided and is used for estimating the initial setting time from the setting time curves i.e., the intersection between the $y=35$ and the setting time curve is projected to the x-axis, and this x-intercept value is taken as the initial setting time. T1, T2 and T3 in Figure 18 refer to the setting time trials 1, 2 and 3 respectively under this case. Box control is the curve that gives the setting time curve of mortar subjected to no current. From Figure 18 and Table 12, the initial setting time for $5A/m^2$, $10A/m^2$ and $20A/m^2$ regimes is 170 minutes, 153 minutes and 144 minutes respectively, while the final setting time of the $5A/m^2$ and $10A/m^2$ is 450 minutes, the final setting time of the $20A/m^2$ regime is 495 minutes. Comparing the setting time results without the influence of current (control box mould) and the pDC regimes, the final setting times are increased by 11.1% for $5A/m^2$ and $10A/m^2$, while a 22.2% increase is seen with the $20A/m^2$ regime while the initial setting times of $5A/m^2$, $10A/m^2$ and $20A/m^2$ show a decrease of 5.5%, 13.8% and 19.44% respectively.

5.2.5 Compressive Strength

In figures 19,20 and 21, the control sample is subject to no current. While DC-05, DC-10 and DC-20 refer to the $5A/m^2$, $10A/m^2$ and $20A/m^2$ DC respectively, AC-05V, AC-10V and AC-15V

refer to the 05V, 10V and 15V AC regimes respectively. pDC-05, pDC-10 and pDC-20 refer to the $5A/m^2$, $10A/m^2$ and $20A/m^2$ pDC regimes respectively. The one-day compressive strength of the DC, AC and pDC regimes obtained by following the research methodology is reported in Figure 19.

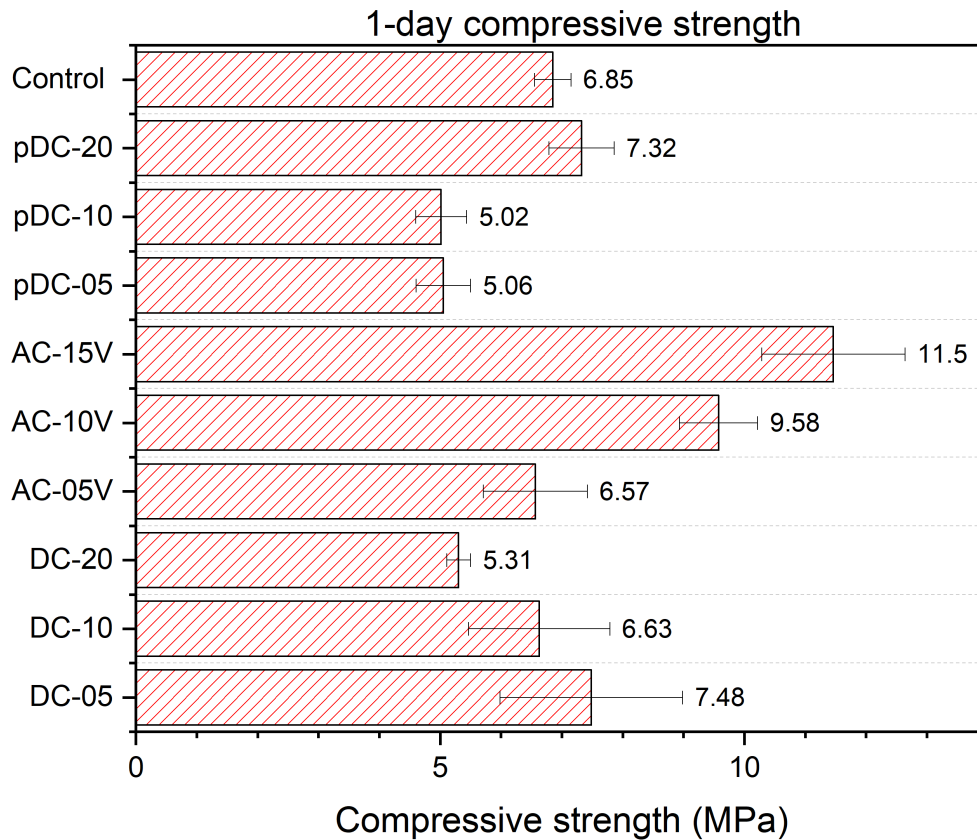


Figure 19: 1-day Compressive strength of all the curing regimes

Figure 19 shows the variation in compressive strengths, along with the standard deviation, of each current regime used in this study. The 1-day compressive strengths of control (without electric curing), $5A/m^2$, $10A/m^2$, and $20A/m^2$ DC regimes are 6.85MPa, 7.48 MPa, 6.63 MPa and 5.31 MPa, respectively, while for 5V, 10V and 15V AC regimes, it is 6.57 MPa, 9.58 MPa and 11.5 MPa respectively. For the pDC regimes of $5A/m^2$, $10A/m^2$ and $20A/m^2$, the strengths are 5.06 MPa, 5.02 MPa and 7.32 MPa, respectively. The samples subjected to the 15V AC regime have the highest compressive strength, while the $10 A/m^2$ pDC has the least compressive strength. The AC regimes show an increase with an increase in voltage intensity, while the DC regimes show a decrease in one-day strength with increasing current density values. The pDC regimes of $5A/m^2$ and $10 A/m^2$ have similar one-day compressive strengths, but $20 A/m^2$ has an increased compressive strength compared to the other pDC regimes. The DC and pDC and the 5V AC specimens have similar one-day compressive strengths in the range of 5MPa - 7.5MPa

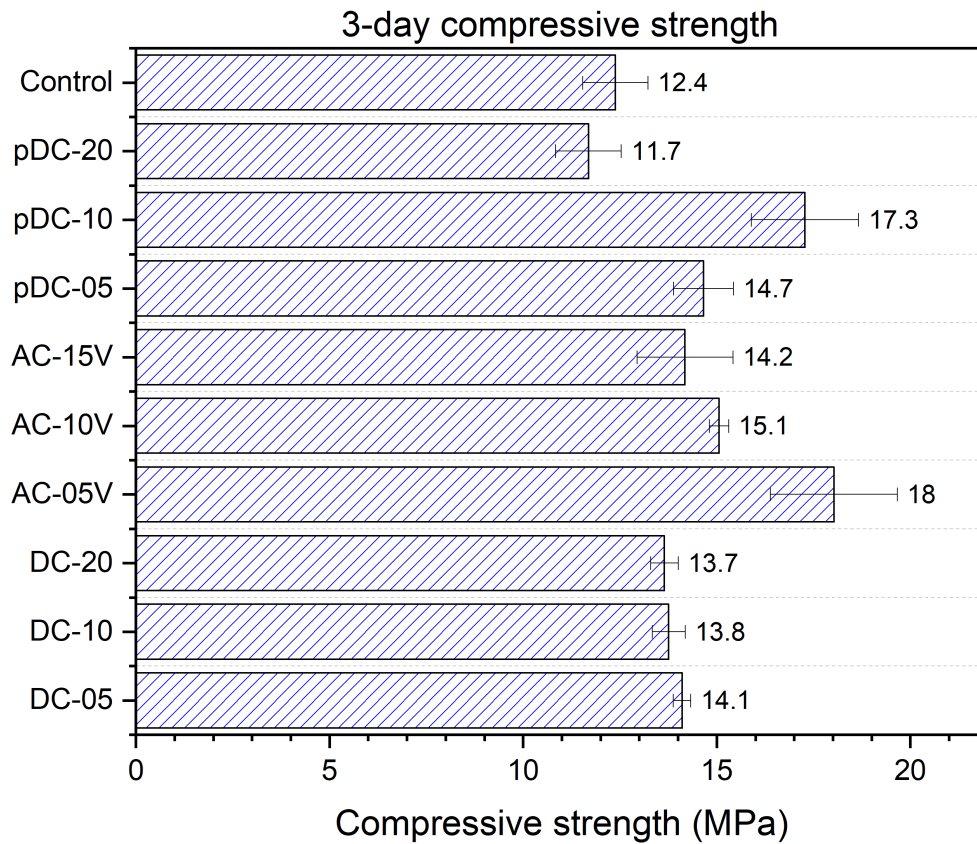


Figure 20: 3-day compressive strength of all curing regimes

Figure 20 shows the variation in 3-day compressive strength between the different current curing regimes. The 3-day compressive strength of $5A/m^2$, $10A/m^2$ and $20A/m^2$ DC regimes are 14.1 MPa, 13.8 MPa, and 13.7MPa, respectively, while for the AC regimes of 5V, 10V and 15V, it is 18.0 MPa, 15.1 MPa and 14.2 MPa respectively. The pDC regimes of $5A/m^2$, $10A/m^2$ and $20A/m^2$ have a 3-day compressive strength of 14.7 MPa, 14.865 MPa and 11.7 MPa, respectively. The strength of the control specimen is 12.4 MPa. The highest compressive strength is that of the 5V AC regime, and the lowest is of the $20 A/m^2$ pDC regime. In the DC, AC and pDC regimes, with the increase in current density/voltage intensity, there is a slight decrease in the compressive strength due to microstructural damage that occurred during the electric curing of the samples.

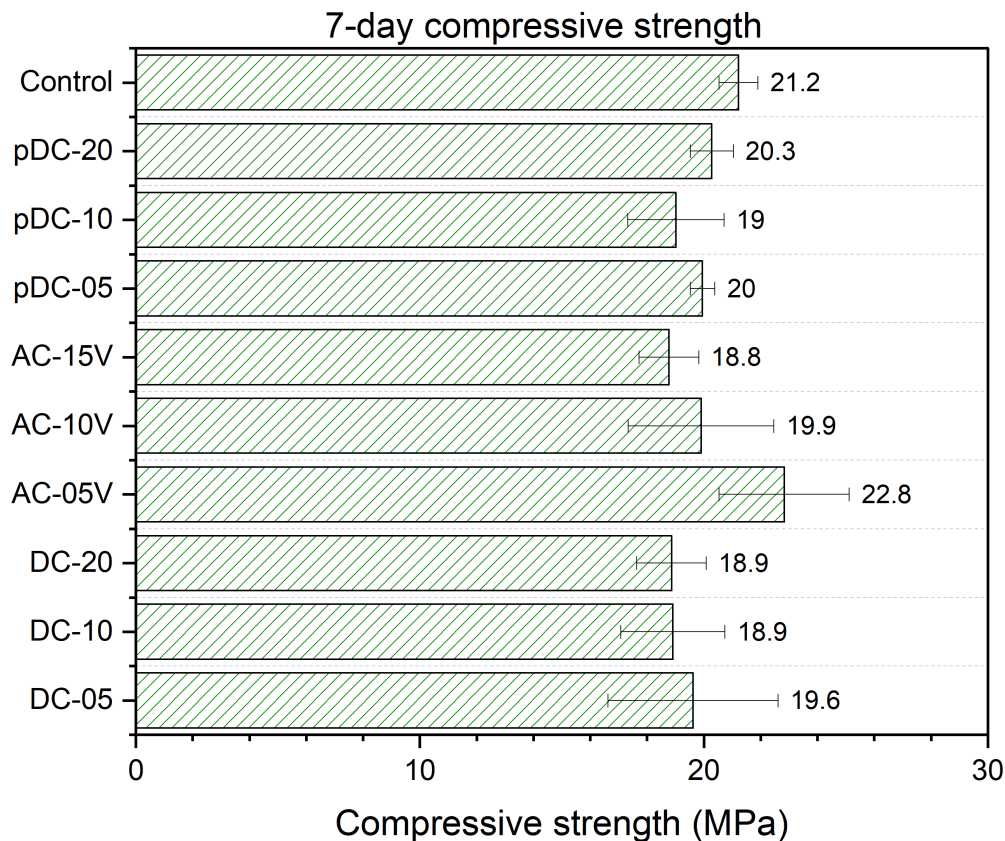


Figure 21: 7-day compressive strength of all the curing regimes

Figure 21 shows the compressive strengths of the different curing regimes used in the methodology. The 7-day compressive strength of the control, $5A/m^2$, $10A/m^2$ and $20A/m^2$ DC regimes are 21.2 MPa, 19.6 MPa, 18.9 MPa, and 18.9 MPa, respectively, while for the AC regimes of 5V, 10V and 15V, it is 22.8 MPa, 19.9 MPa and 18.8 MPa respectively. The pDC regimes of $5A/m^2$, $10A/m^2$ and $20A/m^2$ have a 7-day compressive strength of 20 MPa, 20.3 MPa and 21.2 MPa, respectively. The highest compressive strength is that of the $5A/m^2$ DC regime, and the lowest is of the 15V AC regime. In the DC and AC regimes, the 7-day strength tends to decrease with increasing current density/voltage intensity, mainly due to the microstructural damage that might have occurred during curing. While for the pDC regimes, the compressive strengths vary by approximately ± 1 MPa between them.

5.2.6 Setting Time Vs Resistivity- Direct Current

In this section, setting times and the development of the resistivity of mortar samples subjected to no electric curing and DC curing regimes are obtained following the methodology in section 4. The setting time and resistivity results are reported in Figure 22.

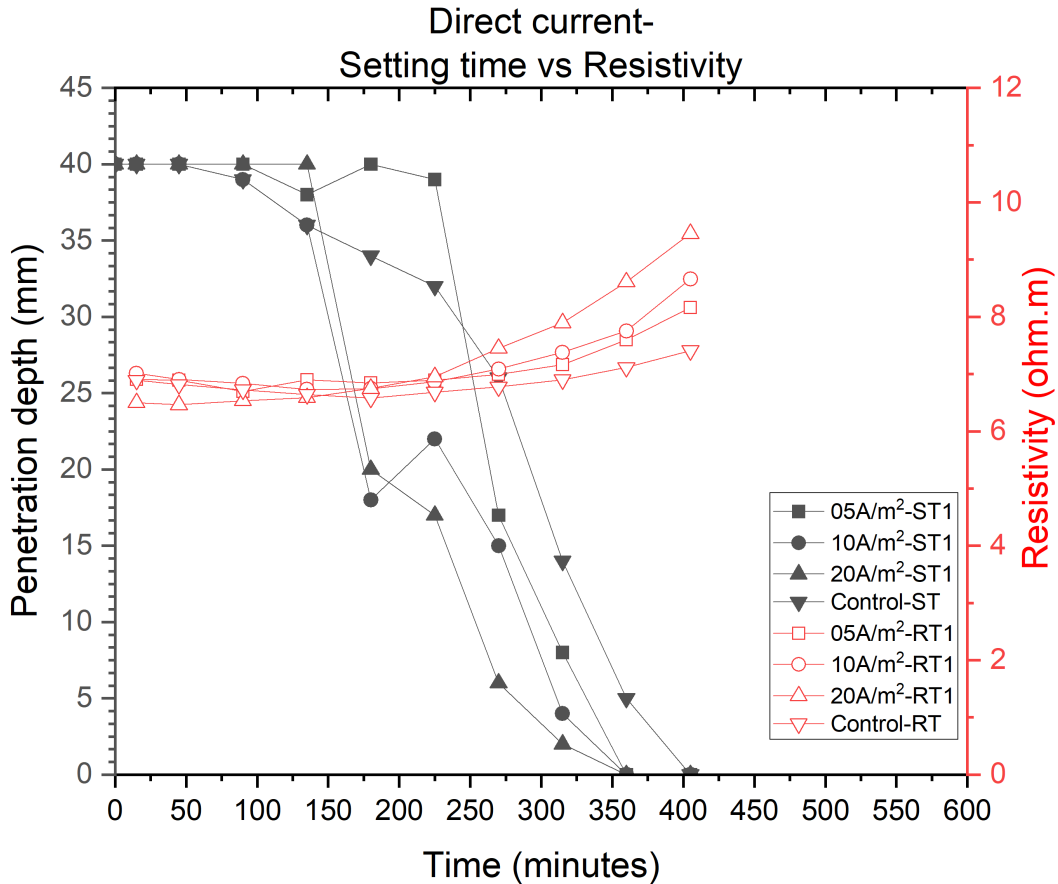


Figure 22: Setting time and resistivity development with time - Control and DC cured specimen

In Figure 22, ST1 refers to the first trial of the setting time test and RT1 refers to the resistivity of the first trial sample. Control ST and control RT refer to the setting time and resistivity measured with the control sample. The setting time and resistivity are measured from the same sample. From Figure 22, (refer appendix-C for the other 2 trials) resistivity develops over time regardless of whether the mortar samples are subjected to electric curing. The resistivity curves also show that the values decrease initially and start to increase after 135-180 minutes mainly due to the formation of hydration products. There is a fluctuation in the resistivity readings for the DC-cured specimens, which could be due to the polarisation of electrodes. For the control specimen, the initial set occurs at 180 minutes while the resistivity curve increases from 225 minutes. After the 135-180 minute period, all the curves show an increase over time. Comparing the resistivity and the setting time curves shows that the increase in resistivity starts when the mortar initially sets.

5.2.7 Setting Time vs Resistivity- Alternating Current

The setting time and the development of resistivity over time of mortar samples subjected to different AC curing regimes are compared with the control specimen and are reported in Figure

23.

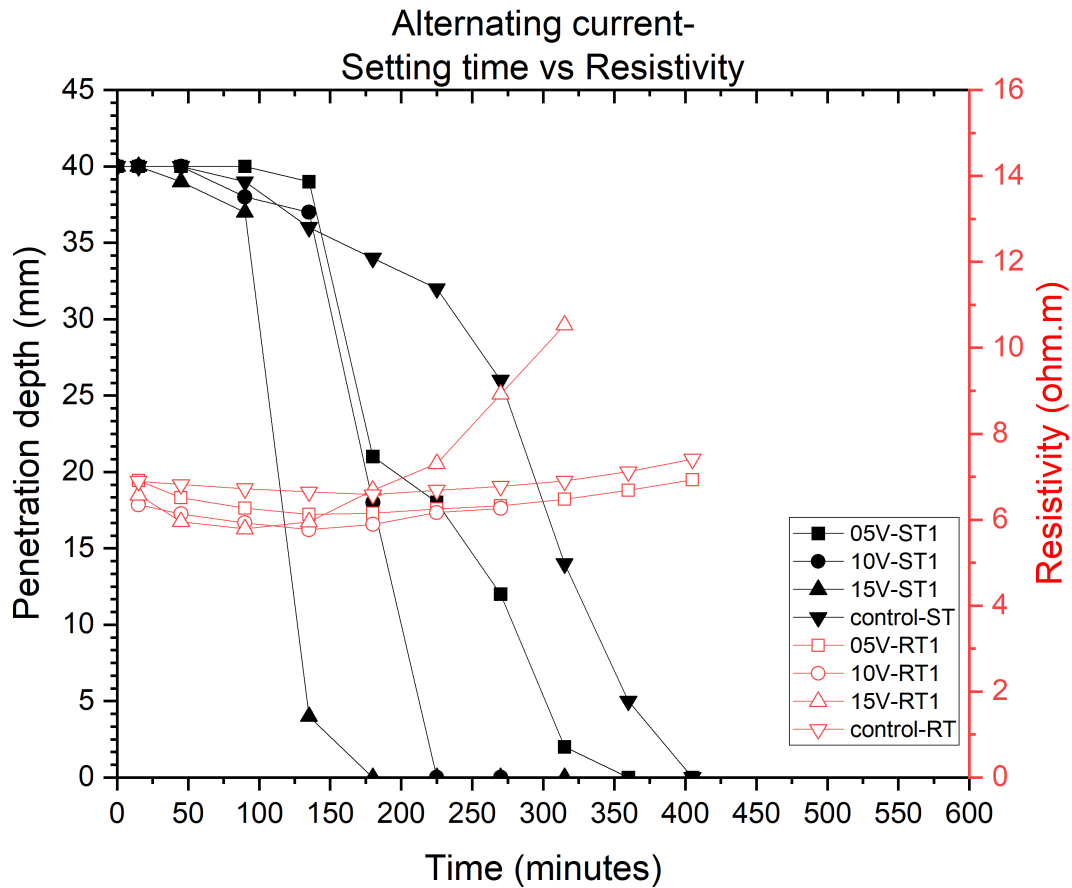


Figure 23: Setting time and resistivity development with time - Control and AC cured specimen

In Figure 23, ST1 refers to the first trial of the setting time test and RT1 refers to the resistivity of the first trial sample. Control ST and control RT refer to the setting time and resistivity measured with the control sample. The setting time and resistivity are measured from the same sample. From Figure 23 (refer appendix-C for the other 2 trials), the trend of decrease in resistivity till the initial set and increase after this point is observed. The control specimen has an initial set of 180 minutes, while the resistivity increases from 225 minutes. For the 5V regime, the initial set occurs at 162 minutes while the resistivity increases from 180 minutes. The coinciding of initial setting time and increase in resistivity is also observed in the 10V and 15V regimes occurring at 139 minutes and 94 minutes, respectively. It is also seen from Figure 16 that the setting of the 10V and 15V samples occur drastically. The resistivity of 15V also increases at a faster rate compared to all the electrical curing regimes.

Voltage regime	Time of initial setting time (mins)	Time of increase in resistivity(mins)
Control	180	180
5V	162	180
10V	139	180
15V	93	135

Table 12: Setting time and resistivity from 23

5.2.8 Setting Time Vs Resistivity- Pulsed Direct Current

The setting time and the development of resistivity over time of mortar samples subjected to pulsed direct current regimes of $5A/m^2$, $10A/m^2$ and $20 A/m^2$, obtained using the methodology reported in section 4, are presented in Figure 24.

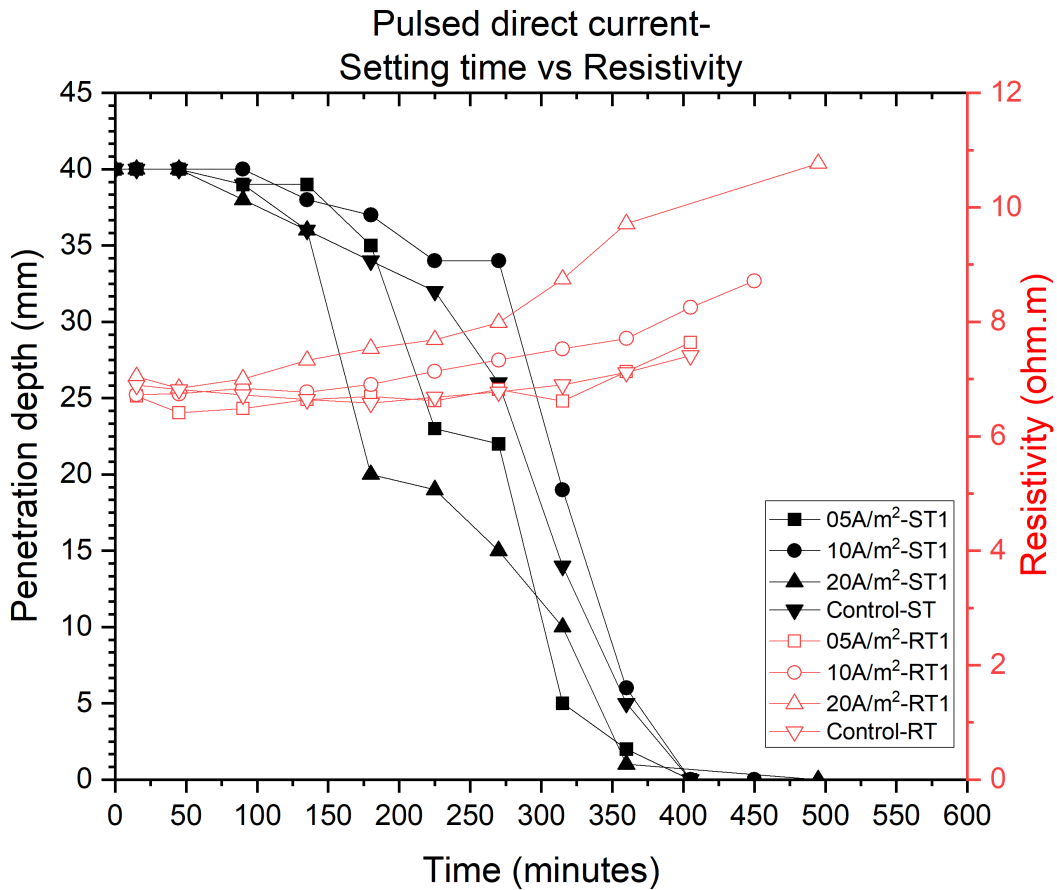


Figure 24: Setting time and resistivity development with time - Control and pDC cured specimen

In Figure 24, ST1 refers to the first trial of the setting time test and RT1 refers to the resistivity of the first trial sample. Control ST and control RT refer to the setting time and resistivity measured with the control sample. The setting time and resistivity are measured from the same

sample. From figure 24 (refer appendix-C for the other 2 trials), the control and the pDC-cured samples show an increase in resistivity over time. However, between the interval readings, the resistivity readings of the pDC samples show fluctuations, i.e., the values do not follow a particular trend of increase or decrease. This fluctuation could be due to the polarisation of the electrodes or due to intermittent direct current during the relaxation period of 5 minutes given before the resistivity readings are taken.

5.2.9 Temperature-Direct Current

In this section, the temperature development recorded using thermocouples of DC regimes $5A/m^2$, $10A/m^2$, and $20 A/m^2$ are represented in Figure 25.

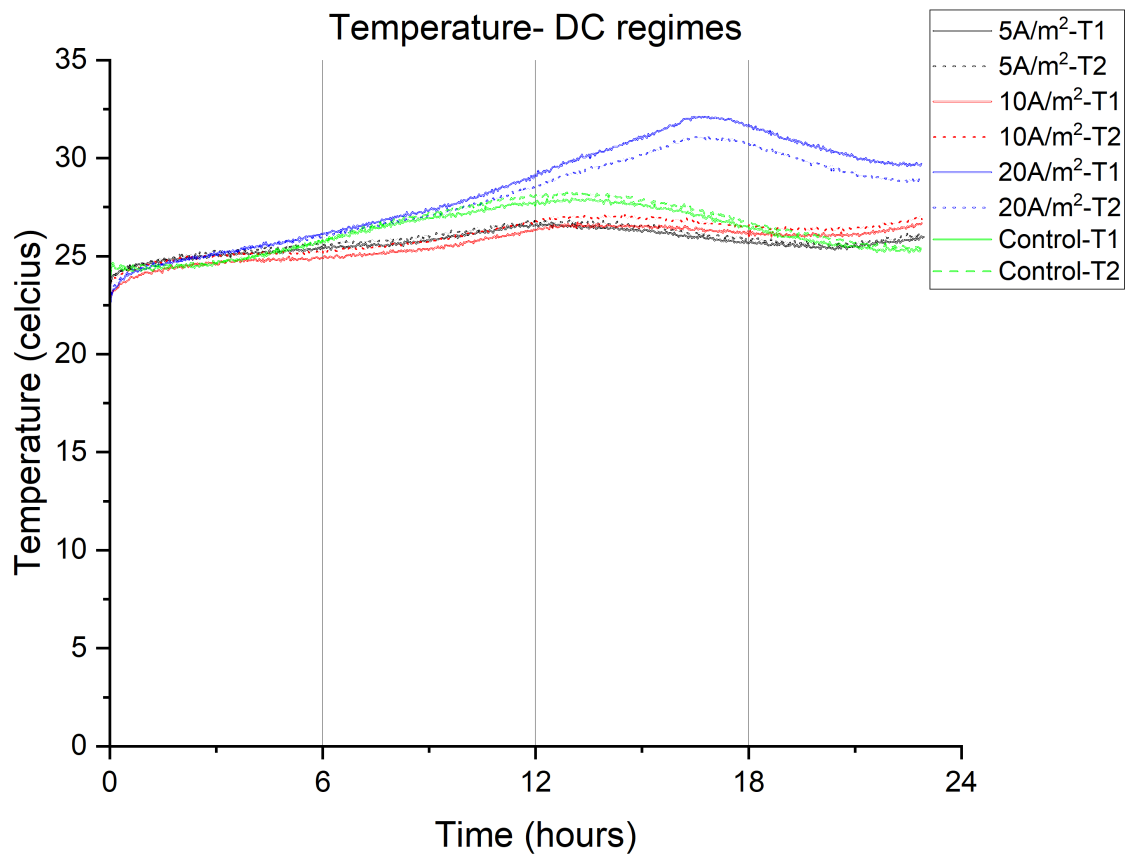


Figure 25: Temperature curves of the selected DC regimes

Figure 25 consists of temperature curves for two trial samples (labelled T1 and T2) from each DC regime and control, and the temperature recordings are done for approximately 24 hours. It is visible that a gradual rise in temperature occurs for the DC regime and the control sample (without electric curing). The temperature peak for all the regimes occurs after approximately 10 hours. An average temperature peak (average of the 2 sample readings) of 28.11°C occurs

approximately after 13 hours for the control sample. For the $5A/m^2$, a peak of 26.8°C occurs at approximately 12 hours, while for $10A/m^2$ and $20A/m^2$, the peaks of 26.9°C and 31.6°C occur at 13.5 hours, 17 hours, respectively. Following the temperature peaks, all the curves gradually decrease and remain constant from that point onwards. Figure 25 also illustrates that the temperature peaks occur after 10 hours, approximately.

5.2.10 Temperature-Alternating Current

The temperature development of 5V and 10V AC regimes are presented in Figure 26. The figure consists of two temperature curves from two samples (labelled T1 and T2) subjected to the AC regime and control samples subjected to no voltage intensity. The figure also compares the temperature development of samples with no electric curing and samples cured with AC regimes.

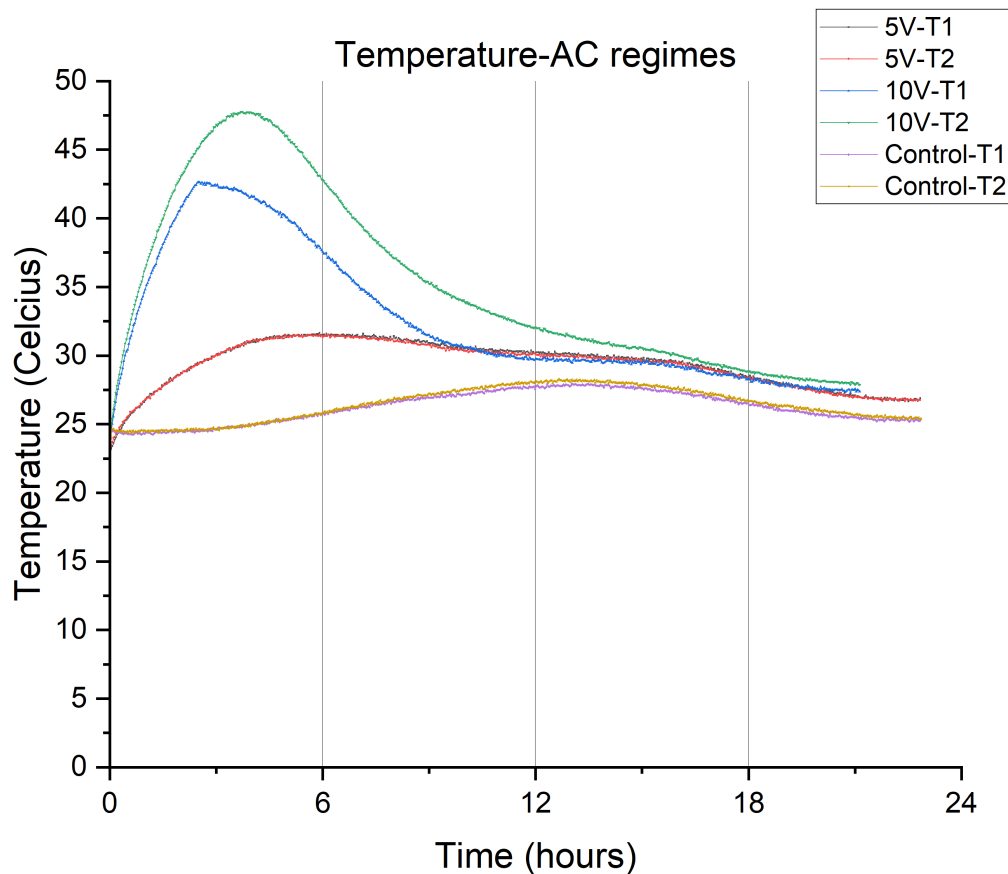


Figure 26: Temperature curves of AC regimes

In Figure 26, there is a prominent temperature peak, in terms of magnitude, for the samples cured under the 10V AC regime, and there is a comparatively smaller temperature peak for the 5V regime. For the 5V regime, the peak has a magnitude of 31.6°C occurring at 6 hours, while for the 10V regime, a peak of 45.20°C is observed at 3 hours. The temperature rise for both AC regimes occurs within the 6-hour timeline.

5.2.11 Temperature vs Resistivity

Figures 27 and 28 depict the temperature vs resistivity development in samples subjected to DC and AC curing regimes respectively. The current regime/voltage intensity (solid lines) in the graph legends followed by aRT refer to average resistivity taken from 3 trial samples while current regime/voltage intensity (dotted lines) followed by avg refer to average temperature from 2 trial samples.

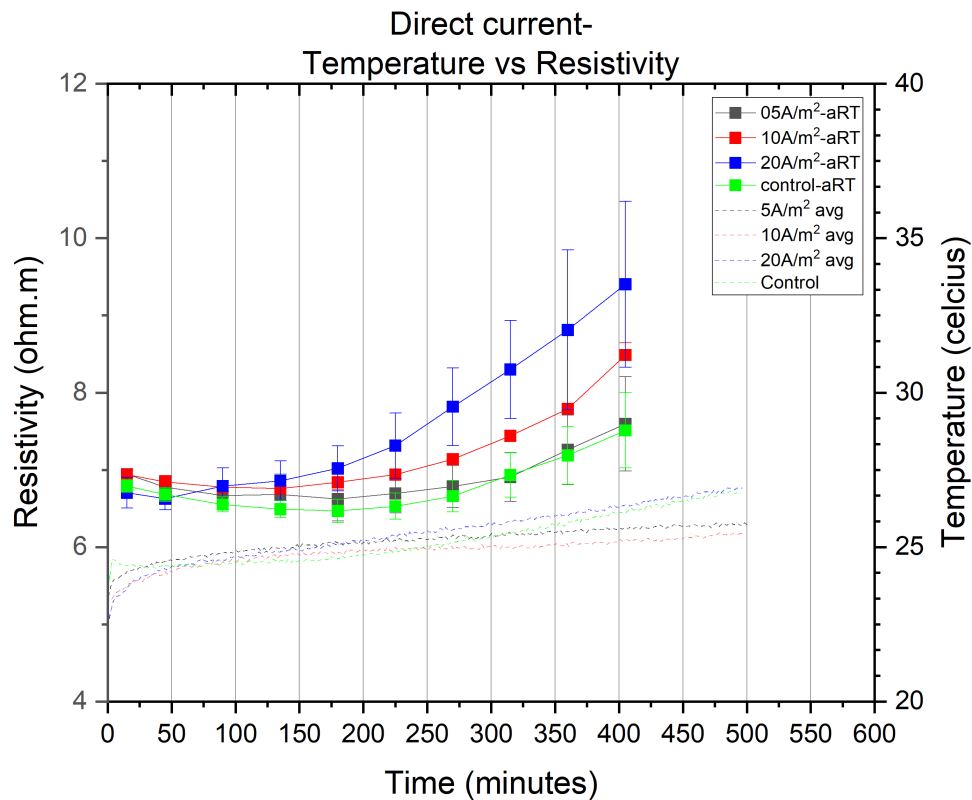


Figure 27: temperature vs resistivity development for DC cured samples

In figure 27, there is an evident increase in temperature and resistivity with the increase in time. Also, between the temperature curves of samples subjected to DC regimes, $20A/m^2$ (highest in terms of the magnitude of current) has the higher maximum temperature evolved at the end of its setting time compared to the $5A/m^2$, $10A/m^2$ and the control. But, from the difference in maximum temperature is less between the $20A/m^2$ regime and the control samples. The samples subjected to $5A/m^2$ and $10A/m^2$ have similar temperature evolution curves. A similar trend is also observed in the resistivity curves, with $20A/m^2$ showing higher resistivity values with an increase in time followed by $10A/m^2$ and $5A/m^2$.

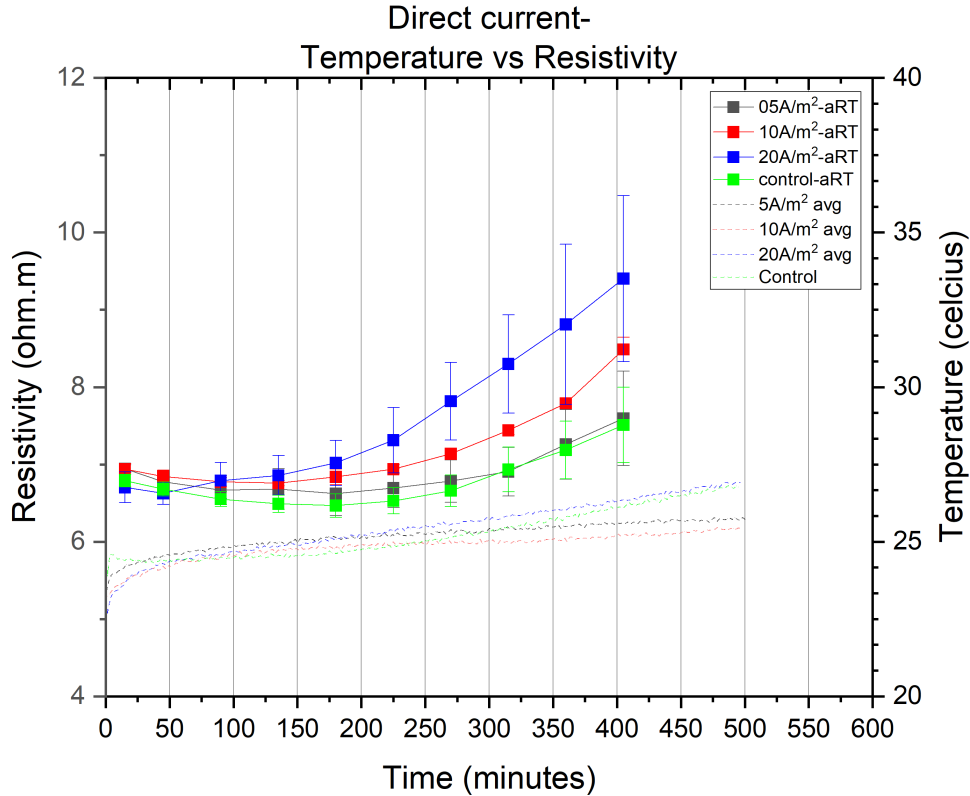


Figure 28: temperature vs resistivity development for AC cured samples

In figure 28, an observation of an increase in resistivity and temperature with time is evident for both the 5V and 10V sample curves. For both the 5V and 10V regime samples, the initial resistivity values are lower and start to increase after 180 minutes (approximately). The resistivity values of 5V and 10V are lower in magnitude when compared to the control while the 15V sample resistivity is lower till 159 minutes and then there is a drastic increase in magnitude.

In both 27 and 28, the increase in resistivity with an increase in temperature could be due to formation of hydration products. Also, with increase in temperature and electric field intensity the ionic concentrations and ionic mobility increases.

5.2.12 Electrical Data- Charges and Power

The charges flowing through the sample subjected to DC or pDC regimes till the final set occurs are reported in Figure 29. The charges presented in Figure 27 are calculated with the data obtained from the software that records data during the curing period. The equation used to calculate electric charge using current is

The theoretical value is obtained by using the formula,

$$Charge = Current * Time \tag{5.1}$$

Where, charge is expressed in coulombs (C)

Current is expressed in ampere (A)

Time is expressed in seconds (sec)

A summary of the electric charges shown in Figure 30 is tabulated in table 13.

Figure 30 provides a graphical visualisation of the electrical power used during the curing process due to passing a current through the sample. Electrical power is calculated with the voltage (V) and current (I) recorded by the software. The equation used to calculate electrical power, represented in Figure 29, is

$$Power = Voltage * Current \quad (5.2)$$

Where, power is expressed as Joule/second or Watt (J/sec or W)

Potential is expressed as voltage (V)

Current is expressed in ampere (A)

A summary of the calculated power values is tabulated in table 14 .

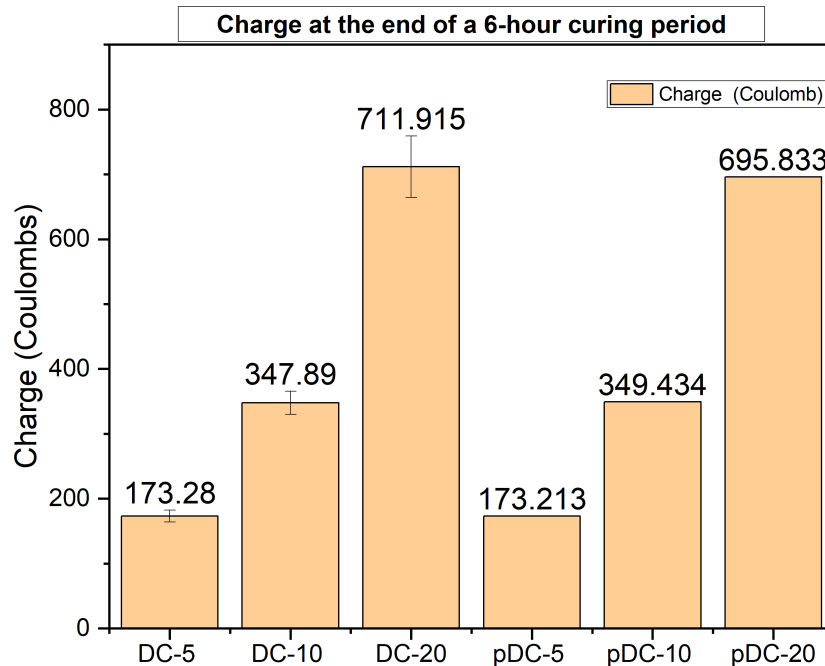


Figure 29: Charge Comparison- DC and pDC regimes

Figure 29 shows that with increasing current densities, there is an increase in the amount of charge that flows through the sample within each current type, i.e., the charge values are higher for the $20A/m^2$ regime DC regime than the $5 A/m^2$ DC regime and the same trend holds for the pDC regimes. The DC regimes of $5A/m^2$, $10A/m^2$ and $20 A/m^2$ (represented as DC-5, DC-10, DC-20 in figure 29) have charge values of 173.28 C, 347.89 C, and 711.915 C, respectively, where C is the unit of charge, Coulombs. Similarly, the pDC regimes of $5A/m^2$, $10A/m^2$ and $20 A/m^2$

(represented as pDC-5, pDC-10, pDC-20 in figure 29) have charges of magnitude 173.21 C, 349.43 C and 695.83 C, respectively. The DC charge values are an average of data from three separate samples, while the pDC charge is obtained by using the data from a single pulse and multiplying it with the time taken for the final set to occur.

Current regime	Charge at the end of a 6-hour curing cycle (Coulomb)
DC-5 ($5 A/m^2$)	173.28
DC-10 ($10 A/m^2$)	347.89
DC-15 ($15 A/m^2$)	711.915
pDC-5 ($5 A/m^2$)	173.213
pDC-10 ($10 A/m^2$)	349.434
pDC-20 ($20 A/m^2$)	695.833

Table 13: The amount of charge the DC/pDC regime supplies at the end of the 6-hour curing cycle

From Figure 29 and Table 13, it is seen that quantification of charges can only be made when the current is direct current or pulsed direct current. Quantification, in terms of charge, would not be relevant even if calculated for AC as the alternating current has a positive and negative phase for current, resulting in a net zero charge.

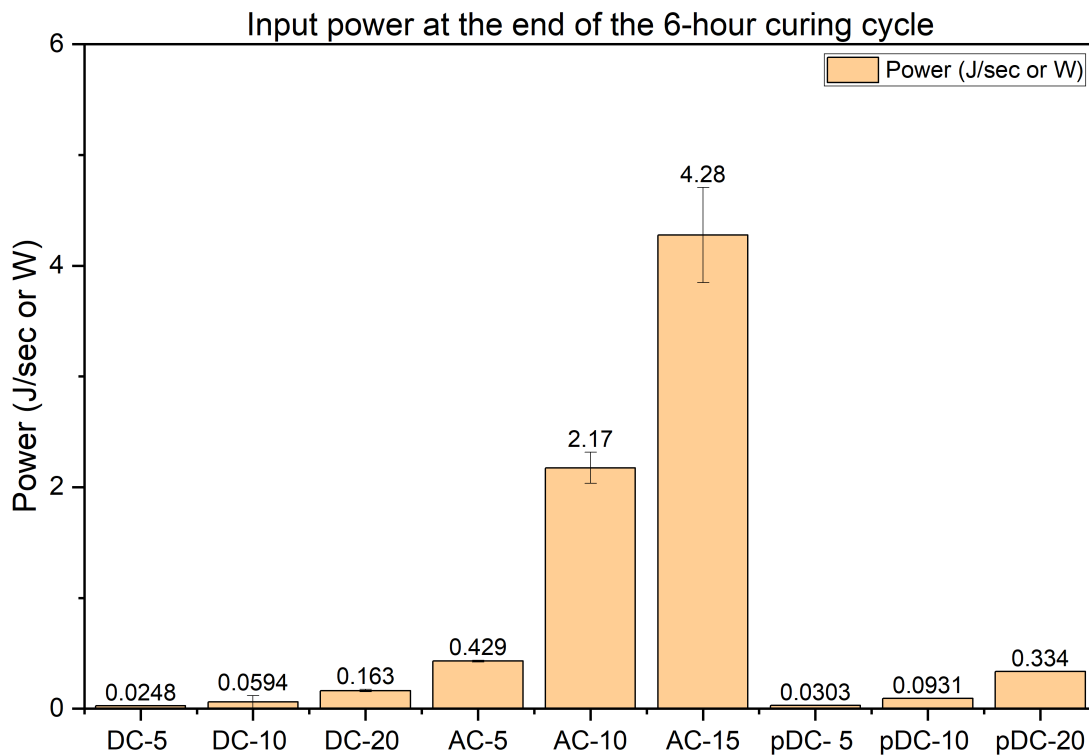


Figure 30: Power Comparison between DC, AC and pDC regimes

Figure 30 shows that the highest input power is applied with the 15V AC regime. The input power for AC regimes 5V, 10V and 15V (represented as AC-5, AC-10 and AC-15 respectively in figure 30) are 0.429 W, 2.17 W and 4.28 W respectively. The input power obtained through applying DC regimes of $5A/m^2$, $10A/m^2$ and $20 A/m^2$ (represented as DC-5, DC-10 and DC-20 in figure 30) are 0.0248 W, 0.0594 W, and 0.163 W, respectively, while for pDC regimes of $5A/m^2$, $10A/m^2$ and $20A/m^2$ (represented as pDC-5, pDC-10 and pDC-20 respectively in figure 30) it is 0.0303 W, 0.0931 W and 0.334 W respectively. Compared to the AC regimes, these values are in the lower bracket because of the lower current densities chosen for the curing cycles. The pDC regimes were chosen to replicate exactly the DC regime in terms of magnitude, but in Figure 30, that is not the case. Each pDC regime has a higher power input than its DC counterpart. A reason for this could be the measurement method used for the assessment of the magnitude of the pulses.

Current regime	Power at the end of the 6-hour curing cycle (J/sec or W)
DC-5 ($5 A/m^2$)	0.0248
DC-10 ($10 A/m^2$)	0.0594
DC-20 ($20 A/m^2$)	0.163
AC-5V	0.429
AC-10V	2.17
AC-15V	4.28
pDC-5 ($5 A/m^2$)	0.0303
pDC-10 ($10 A/m^2$)	0.0931
pDC-20 ($20 A/m^2$)	0.334

Table 14: The amount of charge the DC/pDC regime supplies at the end of the 6-hour curing cycle

Figure 30 and Table 14 show that the input power is the highest in the 15V AC regime since both the voltage and current are of higher magnitude during the initial stages of curing. The pDC regimes are expected to have the same power input as the DC regimes, but it is not the case from the experimental results. Comparing the setting time curves shown in Figures 15, 16 and 18 of DC, AC and pDC regimes, respectively, with Figure 30, it can be reported that the setting time does not necessarily decrease with the increase in power supplied to the sample. For the DC regimes, the effects of increasing power are not reflected in the setting time results. In contrast, for AC regimes, the setting time decreases with an increase in power supplied, and the setting time increases with the increase in power supply in the case of mortar subjected to pDC.

6 Discussions

6.1 Validity of the Experimental Setup

Different types of electrical setups have been established for the curing of cement-based materials with electric current, as reported in [13][24][40][6][42][23] and were designed to monitor temperature, resistivity development with time and compressive strength. The electrodes in these setups were end plates, strip electrodes or bar electrodes made of steel [13], graphite [23] or brass [24] and alternating current was used for curing. The samples were sealed to minimise moisture loss or had a standing water layer to compensate for the evaporating water due to heating. The samples were enclosed in an insulation box [23] to maintain the heat generated by passing current, thus improving the curing efficiency. The current research aims to establish setting time by using a modified vicat apparatus that works on the principle of plunging a needle with a specified mass. So it was not possible to seal the surface. The loss effect was minimised by choosing a smaller sample cross-section enabling to assume that the flow of current lines is uniform and to make use of the size effect, i.e., the heat loss from a sample increases with an increase in the surface area [16].

The selection of a smaller sample size and the choice of not using steel plates as electrodes can be attributed to the usage of direct current for electrical treatment. The choice of titanium MMO meshes was made to minimise corrosion of the electrodes, as the occurrence of corrosion would reduce the efficiency of the flow of current through the sample, and an increase in sample size would have required an increase in electrode size in order to have good electrical contact with the sample. This increase in electrode area would have resulted in higher hydrogen evolution, compared to a smaller electrode area, due to electrolysis when using direct current. The evolution of hydrogen in laboratory conditions is not deemed safe as it is a flammable gas [33] and was kept as a criterion while the curing setup was made.

6.2 Setting Times

Previous study [40] has shown the setting time to be found with temperature curves obtained from thermocouples. In the current study, the setting times were found with a modified vicat apparatus for all the current types and regimes. Setting time values are arbitrary values that signify a reduction in workability (initial) and an increase in solidification (final).

6.2.1 Direct Current

Figure 15 shows that the initial and final setting times of the control and the direct current regimes are the same for the box mould. Comparing the three trials of any regime fluctuations can be observed. For instance, the setting time readings of $10A/m^2$ at the 180th minute are 18, 20 and 24 for the three trials, respectively, while the readings at the 225th minute are 23, 23 and 24, respectively. This discrepancy in the curve could be because of two reasons: i) when the needle of the vicat is dropped, there is a possibility that the needle counters an aggregate particle obstructing the needle along with the added influence of lack of compaction, ii) the application of direct current through an electrolytic sample (ions from cement hydration in water) disrupts the dissolution process and occurs till the hydration products formed are dense enough to withstand

the effects of the passing direct current. The period after the initial setting time is when the sample is in a fluid plastic stage application of a unidirectional current during this period tends to bring about discrepancies in the results. On comparing figures 31 and 32, it can be inferred that with on applying direct current, there is evident hydrogen evolution at the electrodes.



Figure 31: 20 A/m² samples prepared for a 3-day compressive strength test

After the initial set, empty capillary pores are left behind as the free water gets used up, which would later be filled with hydration products. However, the chance of hydrogen gas bubbles getting trapped in these pores, especially near the region immediately surrounding the electrodes, is a possibility that cannot be neglected and may reduce the efficiency of curing since the contact between the electrode and the mortar is reduced. In electric curing/ treatment, the setting time can be reduced if the temperature rise induced due to the application of current increases since the heat produced is proportional to the square of the current applied (Joule law of heating) [22]. On comparing the temperature curves obtained from thermocouple readings (figure 26), there is a slight increase in temperature, but a similar increase is also found for the control samples. Similar temperature values have been reported by Susanto et al. [35]. Susanto et al.[35] have also reported minimal positive impact in applying direct electric current densities below 60 A/m² on hydration reactions.



Figure 32: Control samples (without application of current) prepared for a 3-day compressive strength test

With the setting time and temperature curves (Figure 15,25), the current regimes do not decrease the final setting times because there are no significant temperature development due to the current application within the setting time period. So, it can be added to [35] that setting time, which is related to the reactions of C_3S , C_3A , and C_4AF hydration and subsequent formation of CSH and ettringite, is not significantly changing with current regimes up to $20 A/m^2$.

6.2.2 Pulsed Direct Current

On comparing the setting times of direct current regimes (figure 15) and pulsed direct current regimes (figure 18), the pulsed direct current has a retardant effect on the mortar setting, as the final setting times are in the range of 450-495 minutes, with 495 mins being the final setting time for the $20A/m^2$ regime.

Pulsed DC works like an alternating current source, except that the current magnitude goes to zero (for example, see Figure 11) instead of flowing in the opposite direction. So, it has the effect of DC but a reduced hydrogen evolution. The usage of pulsed current requires the pulse to be of a higher magnitude to get the equivalent of a direct current regime. So, the short pulses of higher magnitude current disrupt the dissolution and the coagulation process of hydration products, could be the reason for the delay in final setting times in the pDC regimes. Another possibility is that the pulse DC leaves the hydration products, which are formed, with surface charges that might repel like charges preventing the coagulation/chain formation of hydration products, as in the case of the mechanism of a retardant or plasticisers.

Except for the $5A/m^2$ pulsed regime, the $10A/m^2$ and $20A/m^2$ regimes fluctuate after the initial set and can be reasoned out to be the same phenomenon that causes the fluctuations in the direct current regimes. However, the effect is profound here compared to its counterpart (DC regime), given the setting time results. (From the device readings, the magnitude of the pulse does not go to zero during the OFF phase due to the slower sampling rate of the recording device)

6.2.3 Alternating Current

Even though alternating current has a different functioning principle, it is widely used for electric curing. The main reason for AC usage is its tendency to minimise electrolysis while passing current through an electrolyte, drastically reducing polarisation and hydrogen evolution at the electrodes.

Unlike direct and pulsed direct current, alternating current regimes render similar results in all the trials. The evolution of heat is also profound with an increase in voltage fields. From the decrease in setting times shown in figure o05, the reactions of C_3S , C_3A , and C_4AF , the critical reactants in hydration product formation that correlate with the setting, occur faster due to the temperature increase. The dissolution of ions also occurs at a higher rate which is revealed as a quantifiable value in compressive strength. The heat occurring due to the passage of AC through the sample renders the cement particles with a denser inner CSH product when compared to the outer CSH. Also, with the increase in temperature, the dissolution of ions results in a supersaturated solution with more ions than a control sample. Thus, resulting in thicker shells of hydration products at early ages [17, 11, 30].

It is understood that the voltage varies with an increase in resistance (Ohm's law), and the same holds for mortar samples. As hydration products form, there is increased resistance to the current flow as the electrolyte (water and dissolved ions) slowly deteriorates, reducing conductivity. This resistance is what makes it possible for the conversion of electric energy to heat energy. Thus, if we assume a constant voltage regime of 15V for experimental purposes, then the current would reduce with the increase in resistance which would, based on Joule's law of heating [22], result in lesser heat evolution and could be the reason why the 5V regime could not show significant temperature rise while 10V and 15V regimes also are subjected to this phenomenon. The resistance occurring within the curing period was not high enough to cause the drop in current. Thus, enabling 10V and 15V regimes to be efficient when it comes to achieving a higher temperature. Also, if it were the curing of the mortar that was the key emphasis, then a factor like temperature would be considered for monitoring the curing. Since reducing the setting time was the key objective achieving high temperature at a short period was focussed on (heating period) than the isothermal period where the retention of that temperature is required.

When chemical accelerators are used (17), the decrease in setting time is mainly achieved by supersaturation of the ionic solution with Ca^{2+} , which facilitates the rapid formation of hydration products. Similarly, an increase in temperature of an electrolytic solution, such as cement paste/cement mortar, with a negative temperature gradient (resistivity decreases with an increase in temperature), i.e., the solution becomes more conductive due to the presence of ionic species. There is a limit to allowing this increased dissolution process, after which crystallisation can occur for a particular current regime. The more saturated the solution, the more the possibility of forming hydration products such as CSH and CH.

6.3 Compressive Strength

6.3.1 Direct Current

A temperature increase when passing a current through the samples would have resulted in an increase in compressive strength because, with an increase in temperature, the occurrence of C_3S reaction happens earlier, resulting in the formation of denser hydration products due to increased dissolution of ions into the solution. It should also be noted that an increase in the current regime does not necessarily mean an increase in compressive strength [40]. The same is supported by the 1-day compressive strength results in Figure 19, where the $20A/m^2$ regime shows lesser strength than the control and the other electrically treated samples. The 1-day strength of $5A/m^2$, $10A/m^2$, and control samples are similar, while the $20A/m^2$ regime has detrimental effects on compressive strength. The 3-day and 7-day compressive strengths (Figure 20 and 21, respectively) of all the DC regimes are similar in magnitude. There is a possibility that the compressive strength of the DC-cured specimens compared to the control can be lesser because accelerated curing tends to leave the microstructure with increased porosity leaving the sample with reduced strength with time.

6.3.2 Pulsed Direct Current

Since, pulse direct current is relatively new in the field of curing, the amount of samples used for the compressive strengths do not provide a certain trend. Thus, a more intensive study is required to come up with a solid discussion. However, with the data obtained a few points have been explained in Appendix-B under Pulsed Direct Current- Compressive Strength.

6.3.3 Alternating Current

When alternating current is passed through the sample, the reaction of C_3S is accelerated, and the subsequent formation of CSH is also accelerated, resulting in higher early-age strengths. An increase in voltage field does not increase in compressive strength with time. It depends on how much heat is generated and how long it is retained. If there is a very high-temperature situation in the sample, then the microstructural damage would be high, resulting in the loss of strength. Thus, emphasising the need to monitor temperature during the curing process [13, 40, 6].

According to Figure 19, showing the one-day strengths, the 5V regime is similar to the control specimen strength. Though the 3-day strength is higher for 5V, the control and 5V specimens show the same compressive strength on the seventh day.

For the 10V samples, decreases in strength as the age of the sample increases. At 7 days, the 10V sample has slightly lesser strength than the control sample. However, it has approximately 80% more compressive strength on the first day than the control sample. The increase can be attributed to the hydration acceleration due to the current application. While the latter reduction in strength can be due to the higher porosity of the sample due to high heat generated during the electrical treatment stage, not only in the microstructure but also having highly porous hydration products.

15V samples are rendered with high temperature, resulting in higher 1-day compressive strength, almost equivalent to the 3-day compressive strength of the control samples. However, it shows a detrimental trend with an increase in the specimen's age owing to higher porosities during the

electric treatment period. The hydration products formed due to increased temperature have dense shells, which should not be confused with the porosities caused in the microstructure [30]. Nevertheless, the presence of hydration products with increased porosities after the treatment period is over should not be overruled.

6.4 Resistivity

6.4.1 Direct Current and Pulsed Direct Current

From Figures 22, the resistivity of the sample tends to increase with time, but till the initial set occurs, there is a decrease in resistivity. The rate at which the decrease occurs, the rate of conductivity, is similar to that of a control sample. If there were an increase in temperature caused due to the application of current, then the conductivity of the ionic solution would have been higher owing to the negative temperature coefficient of an electrolyte. The gradual increase in resistivity is due to the formation of hydration products which render the mortar mix with increased resistance. Transport of ionic species within the pore structure of the cementitious materials occurs due to migration, permeation, absorption and diffusion. The migration of ions is influenced by an application of an external electric field. Therefore, the higher the electric field, the faster the velocity of the ionic species which in turn results in a faster migration. Also, with an increase in temperature, the ionic concentration in the pore solution tends to increase. The resistivity of the sample subjected to DC curing regimes of $5A/m^2$ and $10A/m^2$ are similar to the control specimen resistivity development. This can be justified by saying that the blockage of the pore network (lower tortuosity) by the charges is not profound as in the case of $20A/m^2$ where the resistivity values start to increase from 200 minutes.

Another reason for an increase in resistivity could be that with increased electric fields, the ions tend to migrate towards the electrodes of the opposite charges i.e., cations to the negative terminal and anions towards the positive terminal, this way there is a build of charges near the electrodes, this could also be a reason as to why there is an increase in resistivity with time along with the development of hydration products and increasing tortuosity.

In the case of pulsed direct current and 24, the results do not point towards drawing a definitive conclusion and for this purpose further research is required with regards to pulsed direct current.

6.4.2 Alternating Current

Here, the rate at which the resistivity decreases can be attributed to the negative temperature coefficient of the electrolyte. The resistance decreases with an increase in temperature, but there is a saturation point above which there is no decrease. During this phenomenon, ions' dissolution occurs at a higher rate due to increased temperature. This way, there is the formation of hydration products of higher density and hence an increase in resistance to the current flow with time. Since there could be blockage of the pore network with increased electric fields, the resistivity tends to be higher for the regimes with the evolution of time. Another reason could be that the evaporation of water due to a high-temperature increase could also leave pores without moisture to allow the migration of ions. The curves in Figure 23 also show that the time when the resistance increases are exactly when the initial set occurs.

6.5 Electrical Data Comparisons

The electrical data calculations for charges reveal that the charges flowing through the sample subjected to DC or pDC regimes increase with increasing current densities. Mathematically this is expected as charge calculation involves multiplying the magnitude of the current and the time for which the current is applied. On the other hand, when DC or pDC is used, while the current flow is kept constant, voltage increases with the sample's increasing resistance to ensure that the set current value remains constant. Since the pDC regimes were chosen to be similar to the DC regime in magnitude, the charge flowing through the sample through the curing period is similar with fluctuations rising caused due to the fluctuations in current/voltage values. There is a slight difference in the magnitude because of the readings taken by the measurement device, which is sensitive to slight variations in current. Adding to this, the sampling rate of the measurement device is not fast enough to exactly obtain the current at that instant of time which is in the scale of microseconds.

These minute fluctuations in current/voltage applied are why there is a standard deviation for the measured DC data. This standard deviation is not presented for the pulse DC regime, as the charges were calculated with the current generating one pulse. This current value is multiplied by the total curing period to arrive at the total charge flowing through the sample. This simplification is a result of the drawbacks of the curing setup. Charge calculations for the AC regime, though they can be carried out, would not be of any technical relevance as AC has a positive and negative cycle for voltage and current. Since charge can have both negative and positive values, the net charge over the curing cycle would be zero. Using the IRMS values for charge calculation would lead to the assumption that only the positive cycle is involved while neglecting the negative cycles in the curing period.

The power calculation data in Figure 30 shows that the AC regimes result in higher input power. This is because, for the AC regimes, the voltage was touted to be kept constant throughout the curing cycle. When a voltage is applied to a wet cement mortar sample, due to high pore water content, there is more flow of current and the current decreases with an increase in resistivity of the sample as the voltage is kept constant. Similar to the charge calculations, the input power should have also been the same, but comparing the pDC regime with its equivalent pDC counterpart, there is an increase in the magnitude of pDC power. This could be because the current does not drop exactly to zero magnitudes; thus, residual current results in a voltage across the sample as per the data recordings. The summation of the product of residual current and voltage may add to the power calculations. This can also be why the difference between DC and pDC powers is higher with increasing current regimes.

Comparing the input power and the setting times in Figures 30 and 16, the setting time of the AC regime can also be attributed to the high power supply, i.e., the more the electrical energy is applied, the more the converted heat energy is available for curing. But this does not hold for the DC and pDC regimes, where the setting time is not influenced by the current (DC) application and the setting time is increased (pDC). Thus, the type of current applied is also a parameter that needs to be considered while electrical curing/treatment.

7 Conclusions

The present research investigated the influence of different current types and intensities on cement mortar. For this study, an electrical curing setup was designed and fabricated. The influence on cement mortar subjected to current was investigated by carrying out experiments to measure setting time, compressive strength, resistivity and temperature development. The effect on setting time due to the addition of a chemical accelerator along with subjecting the cement mortar mix to current was also studied. Through the investigations mentioned above, the following conclusions can be drawn:

1. When subjected to direct current, there is no influence of current on the setting time (final) of the mortar specimen as reflected by the vicat apparatus. The control specimen (mortar without electric treatment) and DC-treated cement mortar have similar final setting times of 405 minutes regardless of the value of the initial setting time.
2. The influence of alternating currents on the setting time of cement mortar samples is profound and is dependent on the intensity of applied voltage. While the 5V regime has identical initial and final setting times compared to the control samples (162 minutes and 405 minutes, respectively), the 10V regime renders samples with an initial setting time of 139 minutes and a final setting time of 270 minutes. The 15V AC regime produced mortar specimens with the lowest initial and final setting times of 94 minutes and 180 minutes, respectively. The decrease in setting time can be attributed to the evolution of heat with increasing voltage intensities; heat development is reflected in the thermocouple temperature measurements taken during the curing cycle. The setting time of the mortar mix with the chemical accelerator subjected to 15V has setting time of 90mins (initial) and 135 minutes (final). The faster initial setting time is due to the initial supersaturation of the pore solution with Ca^{2+} ions as a result of using the chemical accelerator and the effect of having a voltage of 15V across the samples.
3. The 1 day, 3 day and 7 day compressive strengths of DC and pDC samples do not show a significant variation as in the case of AC samples where the 1 day compressive strength of the 15V sample is similar to the 3 day compressive strength of the control sample. The AC regimes show decreased 3 day and 7 day compressive strength with increasing voltage intensity within the AC regime group i.e., the 7 day strength of 5V samples are higher than the 15V samples. This decrease in strength is due to microstructural damage caused by the high temperatures developed during electric curing.
4. The resistivity of samples subjected to current and samples not subjected to current show an increase in resistivity with age. During the initial stages of hydration, there is a decrease in resistivity, which can be attributed to the increased mobility of ions and the usage of a water-cement ratio of 0.5.
5. The resistivity values of samples subjected to AC regimes are not affected by electrode polarisation owing to the frequency of AC current. In contrast, the samples subjected to DC and pDC regimes with a relaxation time of 5 minutes had resistivity values that did not stabilise when the reading was taken with the multimeter. This instability could be due to

the polarisation of the electrode, as these were the electrodes used for the application of current to the sample.

6. Comparing the AC setting time and their respective resistivity curves, the resistivity values start to increase from the initial setting time of the mortar; a similar trend of the setting time and resistivity curves is also observed in the control samples.
7. Along with the current intensities, the type of current used for the electric treatment/curing process also affects setting time, compressive strength and resistivity.

8 Recommendations

The following are recommendations that can be considered for future research:

1. Since AC regimes have been shown to reduce the setting times, this can be applied to 3D printing of concrete where there is a need for faster setting of the printed layers. But, the application of the voltages across the printer nozzle is still to be explored. Heating elements can be applied across the nozzle, while at the same time, heating elements can also be placed around the outside surface of the nozzle. This way, even before printing, the nozzle is heated to some extent.
2. The setting time of only cement mortar is taken up in this research; modifying the cement mixes can render results that can further add to the benefits of the 3D printing industry and in-situ repair works.
3. It can be expected that different cement mixes and different mix designs will provide different outcomes with regards to material properties when electrically cured. In case, concrete is used instead of mortar, higher current densities/ voltage intensities are required simply because of the resistance brought about by the presence of coarse aggregates. The water-cement ratio would play a pivotal role in electrical curing. With increase in water-cement ratio, the conductivity of current would increase. But this need not necessarily mean, w/c of 0.4 and below would not render beneficial outcomes when subjected to electric curing. Thus, with regards to mix designs and cement types more research is required.
4. Further microstructure analysis can be carried out while the hydration process is occurring with the impedance spectroscopy technique. Impedance spectroscopy is a non-invasive and non-destructive technique and the impedance spectra of the cementitious sample can render information regarding the pore structure and pore structure connectivity with supporting measurements such as pore fluid conductivity.
5. A more mechanised system for applying electric current is suggested to avoid fluctuations in the set voltage intensity.
6. Initially, applying current to an automated printer would be challenging to set up. Thus, initial tests for the setting of 3D mortar can be done using a mortar gun with a linearised motor.
7. Computer simulations to see the evolution of heat with an increase in electrical current across different geometries can also be worked out.
8. The current/voltage controls were manually done, and a precise supply of current/voltage in terms of magnitude was not possible. The fluctuations are also attributed to the resistors' sensitivity to control the current/voltage.
9. The setting time readings were taken at 45-minute intervals since the specimen size was such that only 9 data points could have been recorded, as comprehensively described in chapter IV under modified vicat.

10. A square geometry is chosen for the experimental purpose, variations due to geometry are still to be explored.
11. The electrodes used were meshes, and it was used such that it had maximum electrical contact with the cement mortar. For future research applying alternating current, it would be interesting to have plates as electrodes which assure proper electrical contact between the electrode and the cementitious mix.

9 Appendix-A- Mixing procedure

The mixing is done in phases:

1. Aggregates are put in the mixing bowl and allowed to be mixed for 30 seconds. Then the mixer is stopped, and the cement is added.
2. The bowl is again placed in the mixer and is started; half the water (the timer is started at this point 'Zero Time' and is used to measure the initial and final setting times) is added. For this, the cement weighed initially should be free of clumps/lumps.
3. Mixing is done for 90 seconds, and within 30 seconds, the bowl is removed to scrape off the materials stuck to the side walls of the mixing bowl and the blade.
4. The mixing bowl is put in the mixer, and the rest of the water is added as soon as the mixer is started. When accelerators are used, the accelerator is added to this half of the water and then with the cement-aggregate mixture. The mixing is done for 60 seconds.

After this, the mixture is immediately transferred to the Vicat mould, which consists of an oiled mould and a non-porous glass base plate. Compaction is done by just tapping along the sides of the mould, and no undue compaction is provided in this case. The surface is evened out, and the penetration readings are taken. The needle is lowered to touch the mortar's surface for the penetration readings. The plunging part is then tightened, eliminating the chances of initial velocity (as per EN-196-3-2016). The plunger is then released. When the needle penetration has ceased, or 30 seconds after the release of the plunger, the reading is noted for the scale (whichever is earlier) (EN-196-3-2016).

The next reading is taken 1mm from the previous reading and made sure that all the readings are evenly spaced out at 1mm from each other to prevent the influence of the previous reading. (EN-196-3-2016)

As per code (EN-196-3-2016), it is mentioned to take readings at convenient and evenly spaced-out time intervals. For the conventional test, till the initial setting of the mixtures, readings are taken at 15-minute intervals, and after the initial set has occurred, the interval is increased to 30 minutes. Each time a penetration reading is taken, the needle is cleaned after being removed from the sample.

When the penetration reading is (6 ± 3) mm, i.e., the distance between the needle tip and the base plate is (6 ± 3) mm, then the time is noted, and the time between the zero time and this recorded time is taken as the initial setting.

Similarly, the time is noted when the needle reading is 0-5mm. The time between the zero time and this time is taken as the final setting*. *A cutting edge is not used here, and the needle penetration is taken as a representation of the final setting time. This methodology is similar to the one used for an automatic setting time test.

10 Appendix-B

10.1 Pulse Direct Current- Compressive Strength

Between the 1-day, 3-day and 7-day compressive strengths of the pDC current regimes, there is an increase in compressive strength with an increase in age. The 1-day and 3-day compressive strengths of all the pDC regimes and control vary by approximately 2MPa. At 7 days, the compressive strength of the control, though not profound, shows an increase in strength gain compared to the other pDC regimes. The decrease in strength gain of the pDC regimes at 7 days can be due to the intensity of the pulses applied to the fresh mortar causing the improper coagulation of hydration products, or even due to porosities due to hydrogen gas (a mechanism similar to air entrainment). The hypothesis that there could be a possible charge around the hydration products hindering the development can also be a reason.

10.2 Pulse Direct Current- Pulse data

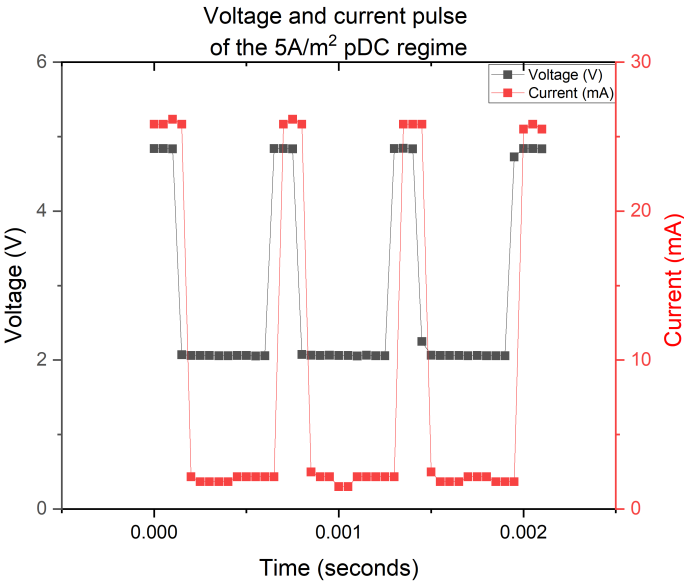


Figure 33: 5 A/m² pDC voltage and current pulse

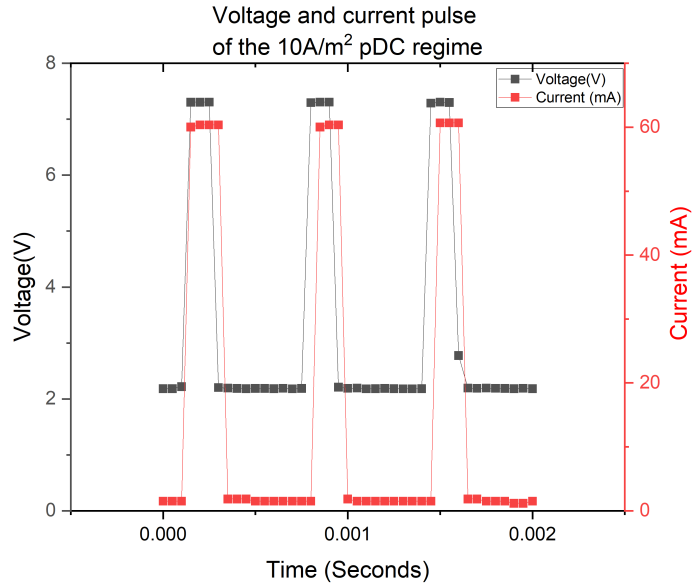


Figure 34: 10 A/m² pDC voltage and current pulse

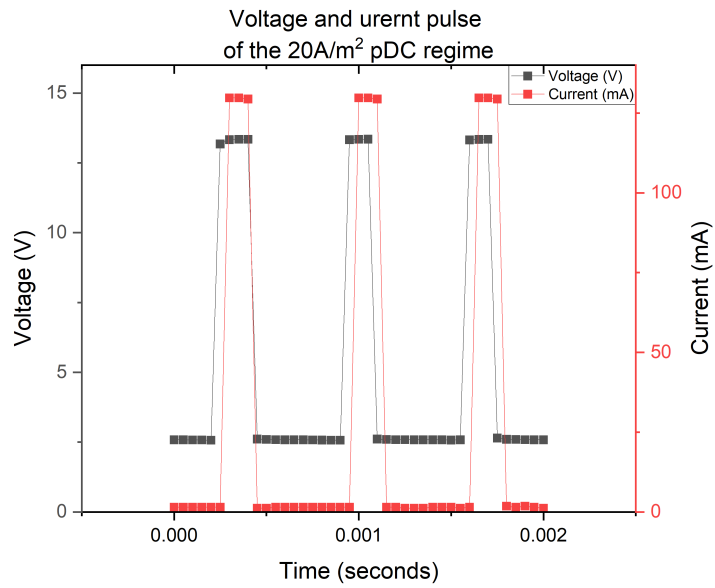


Figure 35: 20 A/m² pDC voltage and current pulse

11 Appendix-C- Setting time vs resistivity

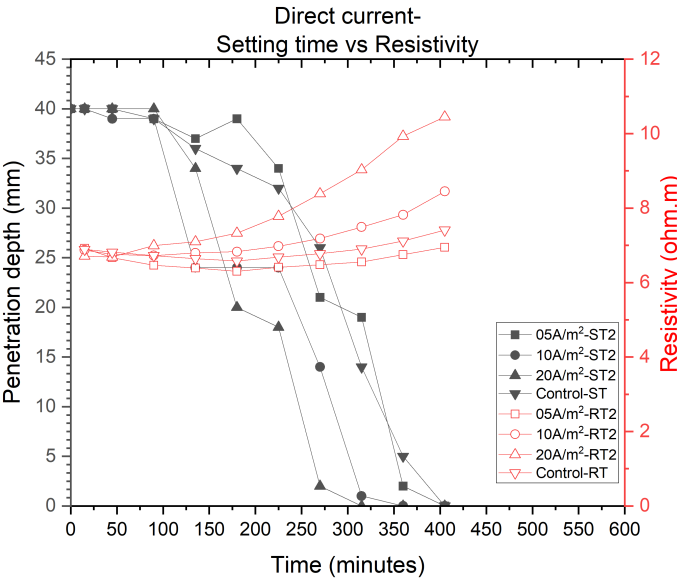


Figure 36: Setting time and resistivity development with time - Control and DC cured specimen- Trial 2

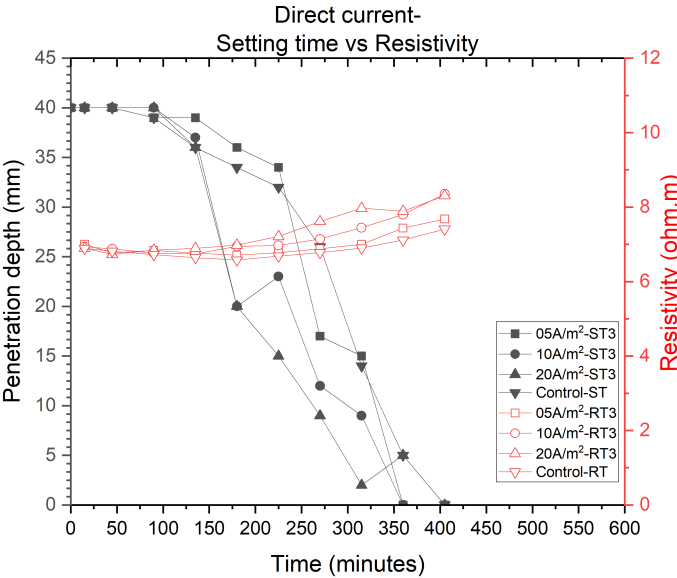


Figure 37: Setting time and resistivity development with time - Control and DC cured specimen- Trial 3

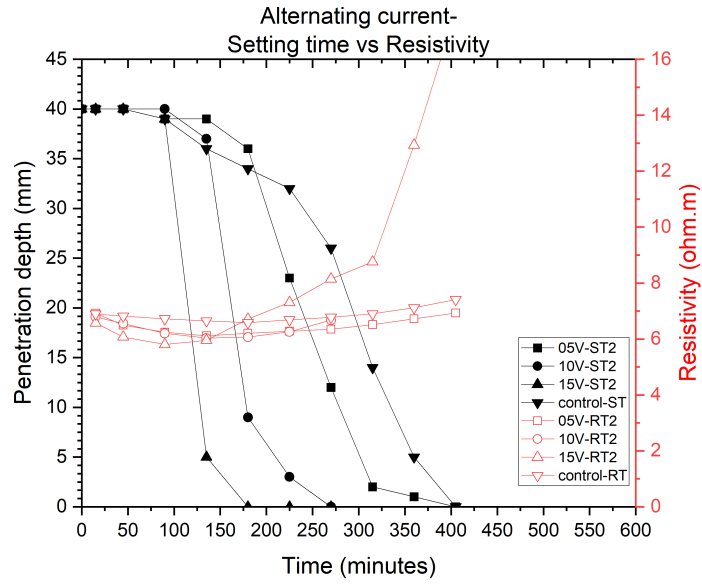


Figure 38: Setting time and resistivity development with time - Control and AC cured specimen- Trial 2

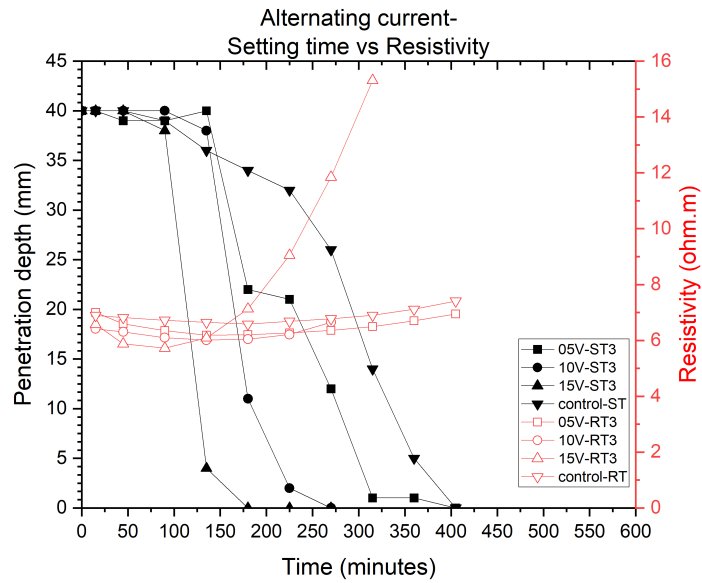


Figure 39: Setting time and resistivity development with time - Control and AC cured specimen- Trial 3

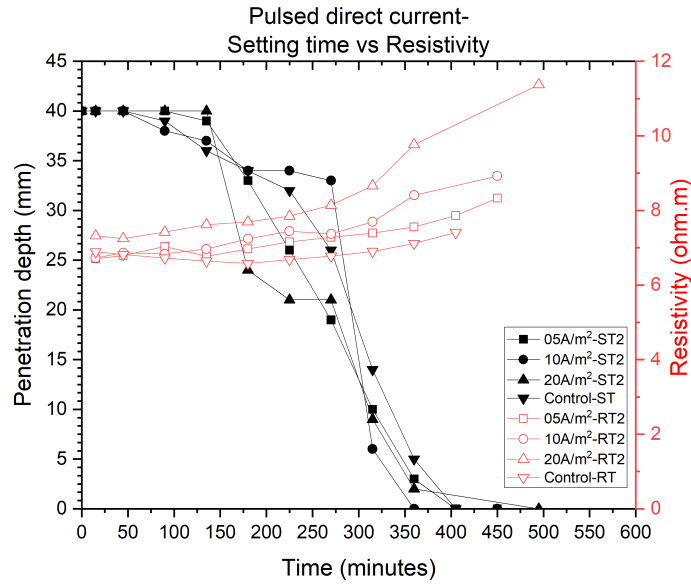


Figure 40: Setting time and resistivity development with time - Control and pDC cured specimen- Trial 2

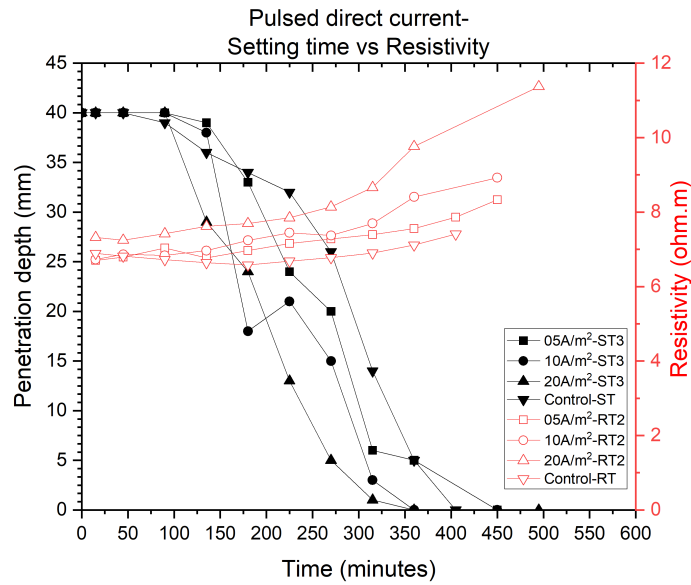


Figure 41: Setting time and resistivity development with time - Control and pDC cured specimen- Trial 3

References

- [1] .
- [2] S. Aggoun et al. “Effect of some admixtures on the setting time and strength evolution of cement pastes at early ages”. In: *Construction and Building Materials* 22 (2 2008-2), 106–110. DOI: 10.1016/j.conbuildmat.2006.05.043.
- [3] A. Bajza and I. Rouseková. “Effect of heat treatment conditions on the pore structure of cement mortars”. In: *Cement and Concrete Research* 13 (5 1983-9), pp. 747–750. DOI: 10.1016/0008-8846(83)90067-4.
- [4] P.I. Banea. “The study of electrical resistivity of mature concrete”. In: (2015).
- [5] L Bertolini et al. *Corrosion of Steel in Concrete : Prevention, Diagnosis, Repair*. Erscheinungsort Nicht Ermittelbar: Wiley-Vch Verlag GmbH, 2013.
- [6] S. Bredenkamp, K. Kruger, and G. L. Bredenkamp. “Direct electric curing of concrete”. In: *Magazine of Concrete Research* 45 (162 1993-3), pp. 71–74. DOI: 10.1680/macr.1993.45.162.71.
- [7] N. Chikh et al. “Effects of calcium nitrate and triisopropanolamine on the setting and strength evolution of Portland cement pastes”. In: *Materials and Structures* 41 (1 2007-1), pp. 31–36. DOI: 10.1617/s11527-006-9215-8.
- [8] *Design and Control of Concrete Mixtures*.
- [9] S Ekolu. *HEAT CURING PRACTICE IN CONCRETE PRECASTING TECHNOLOGY -PROBLEMS AND FUTURE DIRECTIONS*.
- [10] W. Elkey and E. Sellevold. “Electrical Resistivity of Concrete”. In: *Norwegian Road Research Laboratory* (1995).
- [11] I. Elkhadiri and F. Puertas. “The effect of curing temperature on sulphate-resistant cement hydration and strength”. In: *Construction and Building Materials* 22 (7 2008-7), pp. 1331–1341. DOI: 10.1016/j.conbuildmat.2007.04.014.
- [12] Earl D Gates. *Introduction to basic electricity and electronics technology*. Clifton Park, N.Y.: Delmar/Cengage Learning, 2014.
- [13] Ian Heritage. *Direct electric curing of mortar and concrete*. 2001. URL: `\url{https://www.napier.ac.uk/~media/worktribe/output-276402/heritagemortarpdf.pdf}`.
- [14] T.-C. Hou and J. Lynch. “Conductivity-based strain monitoring and damage characterization of fiber reinforced cementitious structural components”. In: () .
- [15] Harald Justnes, Arne Tor, and Hammer. *SINTEF REPORT COIN P1 Advanced cementing materials SP 1.2 F Controlling hydration development Accelerating admixtures for concrete State of the art SINTEF Building and Infrastructure COIN -Concrete Innovation Centre Concrete Betong SELECTED BY AUTHOR Accelerator Akselerator Cement Sement Hydration Hydratisering*.
- [16] I D Kafry. *Direct electric curing of concrete : basic design*. 1993.

- [17] Rachel J. Kjellsen Knut O. and Detwiler and Odd E. Gjrv. "Pore structure of plain cement pastes hydrated at different temperatures". In: *Cement and Concrete Research* 20 (6 1990-11), pp. 927–933. DOI: 10.1016/0008-8846(90)90055-3.
- [18] Guo Z. van Breugel K. Koleva D.A. and J.H.W de Wit. "Microstructural properties of the bulk matrix and the steel/cement paste interface in reinforced concrete, maintained in conditions of corrosion and cathodic protection". In: *Materials and Corrosion* 61 (7 2009), 561–567. DOI: 10.1002/maco.200905423.
- [19] Prsente Le. *Hydration of C 3 A with Calcium Sulfate Alone and in the Presence of Calcium Silicate THSE N O 5035 (2011) COLE POLYTECHNIQUE FDRALE DE LAUSANNE*.
- [20] Thanakorn Leung Christopher K.Y. and Pheeraphan. "Determination of optimal process for microwave curing of concrete". In: *Cement and Concrete Research* 27 (3 1997-3), pp. 463–472. DOI: 10.1016/s0008-8846(97)00015-x.
- [21] Zongjin Li. *Advanced concrete technology*. Hoboken, N.J.: Wiley, 2011.
- [22] Marco Liebscher et al. "Electrical Joule heating of cementitious nanocomposites filled with multi-walled carbon nanotubes: role of filler concentration, water content, and cement age". In: *Smart Materials and Structures* 29 (12 2020-11), p. 125019. DOI: 10.1088/1361-665x/abc23b.
- [23] C. Ma et al. "An effective method for preparing high early-strength cement-based materials: The effects of direct electric curing on Portland cement". In: *Journal of Building Engineering* 43 (2021-11), p. 102485. DOI: 10.1016/j.jobe.2021.102485.
- [24] J .D McIntosh. "Electrical curing of concrete". In: *Magazine of Concrete Research* 1 (1 1949-1), pp. 21–28. DOI: 10.1680/macr.1959.1.1.21.
- [25] Nicolas Muller and Jochen Harnisch. *A blueprint for a climate friendly cement industry*. http://www.environmentportal.in/files/english_report_lr_pdf.pdf. WWF International, 2008.
- [26] Mehta N K and Paulo J M Monteiro. *Concrete : microstructure, properties, and materials*. New York, Ny: Mcgraw-Hill, 2006.
- [27] *NEN-EN 196-3: Determination of Setting times and soundness*.
- [28] A M Neville. *Properties of concrete. 2.ed*. London: Pitman, Repr, 1973.
- [29] Adam M Neville and J J Brooks. *Concrete technology*. Harlow, England ; New York: Prentice Hall.
- [30] C.H. Patel H.H. and Bland and A.B. Poole. "The microstructure of concrete cured at elevated temperatures". In: *Cement and Concrete Research* 25 (3 1995-4), pp. 485–490. DOI: 10.1016/0008-8846(95)00036-c.
- [31] Andrade C. Elsener B. Vennesland . Gulikers J. Weidert R. Polder R. and M. Raupach. "Test methods for on site measurement of resistivity of concrete". In: *Materials and Structures* 33 (10 2000), 603–611. DOI: 10.1007/bf02480599.

- [32] O. Sengul. “Factors affecting the electrical resistivity of concrete”. In: *Nondestructive Testing of Materials and Structures* (2011), 263–269. DOI: 10.1007/978-94-007-0723-8_38.
- [33] *Spontaneous ignition of hydrogen Literature Review RR615 Research Report*.
- [34] A Susanto. “The effect of stray current on hardening and hardened cement-based materials”. In: (). DOI: <https://doi.org/10.4233/uuid:25de1e90-f586-4973-8f04-f2c744609959>.
- [35] A Susanto et al. “Electrical Current Flow and Cement Hydration: Implications on Cement-Based Microstructure”. In: *International Journal of Structural and Civil Engineering Research* (2017), pp. 75–82. DOI: 10.18178/ijscer.6.2.75-82.
- [36] Harry F W Taylor. *Cement chemistry*. London: London Telford Publ.
- [37] P. Taylor H. F. W. and Barret et al. “The hydration of tricalcium silicate”. In: *Materials and Structures* 17 (6 1984-11), pp. 457–468. DOI: 10.1007/bf02473986.
- [38] J.D Thomas N.L. and Birchall. “The retarding action of sugars on cement hydration”. In: *Cement and Concrete Research* 13 (6 1983-11), pp. 830–842. DOI: 10.1016/0008-8846(83)90084-4.
- [39] Selcuk Türkel and Volkan Alabas. “The effect of excessive steam curing on Portland composite cement concrete”. In: *Cement and Concrete Research* 35 (2 2005-2), pp. 405–411. DOI: 10.1016/j.cemconres.2004.07.038.
- [40] İsmail Uygunoğlu Tayfun. and Hocaoğlu. “Effect of electrical curing application on setting time of concrete with different stress intensity”. In: *Construction and Building Materials* 162 (2018-2), pp. 298–305. DOI: 10.1016/j.conbuildmat.2017.12.036.
- [41] Brent Vollenweider. “Various Methods of Accelerated Curing for Precast Concrete Applications, and Their Impact on Short and Long Term Compressive Strength”. In: (2004).
- [42] S. S. Wadhwa et al. “Direct electric curing of in situ concrete”. In: *Batiment International, Building Research and Practice* 15 (1-6 1987-1), pp. 97–101. DOI: 10.1080/09613218708726799.
- [43] S. Wen and D.D.L. Chung. “Electric polarization in carbon fiber-reinforced cement”. In: *Cement and Concrete Research* 31 (1 2001), 141–147. DOI: 10.1016/s0008-8846(00)00382-3..
- [44] John Gibb Wilson and Narendra Kumar Gupta. “Equipment for the investigation of the accelerated curing of concrete using direct electrical conduction”. In: *Measurement* 35 (3 2004-4), pp. 243–250. DOI: 10.1016/j.measurement.2003.11.002.
- [45] N B Winter. *Understanding cement : an introduction to cement production, cement hydration and deleterious processes in concrete*. United Kingdom: Micranalysis Consultants Ltd.
- [46] Huang R. Chi M. Wu T. and T. Weng. “A study on electrical and thermal properties of conductive concrete”. In: *Computers and Concrete* 12 (3 2013), 337–349. DOI: 10.12989/cac.2013.12.3.337.

- [47] Renhe Yang et al. “Delayed ettringite formation in heat-cured Portland cement mortars”. In: *Cement and Concrete Research* 29 (1 1990-1), pp. 17–25. DOI: 10.1016/S0008-8846(98)00168-9.